

Accepted Manuscript

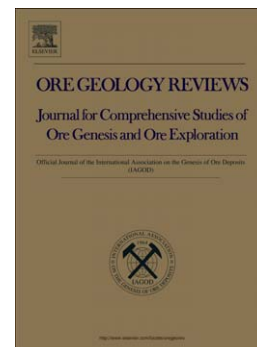
Geochemical differences between subduction- and collision-related copper-bearing porphyries and implications for metallogenesis

JianLin Chen, JiFeng Xu, BaoDi Wang, ZhiMing Yang, JiangBo Ren, HongXia Yu, Hongfei Liu, Yuexing Feng

PII: S0169-1368(15)00024-4
DOI: doi: [10.1016/j.oregeorev.2015.01.011](https://doi.org/10.1016/j.oregeorev.2015.01.011)
Reference: OREGEO 1429

To appear in: *Ore Geology Reviews*

Received date: 25 March 2014
Revised date: 26 December 2014
Accepted date: 14 January 2015



Please cite this article as: Chen, JianLin, Xu, JiFeng, Wang, BaoDi, Yang, ZhiMing, Ren, JiangBo, Yu, HongXia, Liu, Hongfei, Feng, Yuexing, Geochemical differences between subduction- and collision-related copper-bearing porphyries and implications for metallogenesis, *Ore Geology Reviews* (2015), doi: [10.1016/j.oregeorev.2015.01.011](https://doi.org/10.1016/j.oregeorev.2015.01.011)

This is a PDF file of an unedited manuscript that has been accepted for publication. As a service to our customers we are providing this early version of the manuscript. The manuscript will undergo copyediting, typesetting, and review of the resulting proof before it is published in its final form. Please note that during the production process errors may be discovered which could affect the content, and all legal disclaimers that apply to the journal pertain.

Geochemical differences between subduction- and collision-related copper-bearing porphyries and implications for metallogenesis

JianLin Chen, JiFeng Xu

*State Key Laboratory of Isotope Geochemistry, Guangzhou Institute of Geochemistry, Chinese Academy of Sciences,
511 Kehua Street, Tianhe District, Guangzhou, 510640, China
CAS Center for Excellence in Tibetan Plateau Earth Sciences, Beijing 100101, China*

BaoDi Wang

*Chengdu Institute of Geology and Mineral Resources
2 Northern Section of First Ring Road, Chengdu, 610081, China*

ZhiMing Yang

*Institute of Geology, Chinese Academy of Geological Science,
26 Baiwanzhuang Road, Beijing 100037, PR China*

JiangBo Ren, HongXia Yu

*State Key Laboratory of Isotope Geochemistry, Guangzhou Institute of Geochemistry, Chinese Academy of Sciences,
511 Kehua Street, Tianhe District, Guangzhou, 510640, China*

Hongfei Liu

*Tibet Institute of Geological Survey,
21 Beijing Road, Lhasa 850000, China*

Yuexing Feng

*School of Earth Sciences, The University of Queensland,
St Lucia, Qld 4072, Australia*

Abstract Porphyry Cu (–Mo–Au) deposits occur not only in continental margin–arc settings (subduction-related porphyry Cu deposits, such as those along the eastern Pacific Rim (EPRIM)), but also in continent–continent collisional orogenic belts (collision-related porphyry Cu deposits, such as those in southern Tibet). These Cu-mineralized porphyries, which develop in contrasting tectonic settings, are characterized by some different trace element (e.g., Th, and Y) concentrations and their ratios (e.g., Sr/Y, and La/Yb), suggesting that their source magmas probably developed by different processes. Subduction-related porphyry Cu mineralization on the EPRIM is associated with intermediate to felsic calc-alkaline magmas derived from primitive basaltic magmas that pooled beneath the lower crust and underwent melting, assimilation, storage, and homogenization (MASH), whereas K-enriched collision-related porphyry Cu mineralization was associated with underplating of subduction-modified basaltic materials beneath the lower crust (with subsequent transformation into amphibolites and eclogite amphibolites), and resulted from partial melting of the newly formed thickened lower crust. These different processes led to the collision-related porphyry Cu deposits associated with adakitic magmas enriched by the addition of melts, and the subduction-related porphyry Cu deposits associated with magmas comprising all compositions between normal arc rocks and adakitic rocks, all of which were associated with fluid-dominated enrichment process.

In subduction-related Cu porphyry magmas, the oxidation state (fO_2), the concentrations of chalcophile metals, and other volatiles (e.g., S and Cl), and the abundance of water were directly controlled by the composition of the primary arc basaltic magma. In contrast, the high Cu concentrations and fO_2 values of collision-related Cu porphyry magmas were indirectly derived from subduction modified magmas, and the large amount of water and other volatiles in these magmas were controlled in part by partial melting of amphibolite derived from arc basalts that were underplated beneath the lower crust, and in part by the contribution from the rising potassic and ultrapotassic magmas. Both subduction- and collision-related porphyries are enriched in potassium, and were associated with crustal thickening. Their high K_2O contents were primarily as a result of the inheritance of enriched mantle components and/or mixing with contemporaneous ultrapotassic magmas.

Key words: Geochemistry; subduction- and collision-related; Cu-bearing porphyry; eastern

Pacific Rim; southern Tibet.

1 Introduction

Porphyry Cu deposits are the world's main source of Cu as well as a source of significant amounts of Mo and Au; as such, these deposits have been the focus of a large amount of research, both theoretical and applied (e.g., Sillitoe, 1972, 1973, 1998, 2000, 2005, 2010; Richards, 2003, 2009, 2011a, b, 2013; Hou et al., 2004, 2009, 2011; Richards and Kerrich, 2007; Sun et al., 2013). Typical porphyry Cu deposits occur in subduction-related continental and island arc settings, such as those of the Pacific Rim, which are closely associated with the subduction of oceanic crust (e.g., Kelson et al., 1975; Skewes and Stern, 1995; Kirkham, 1998; Kay et al., 1999; Kerrich et al., 2000; Richards et al., 2001). The classic model of porphyry Cu mineralization (e.g., Sillitoe, 1972), which is based on porphyry deposits formed in arc settings, has been the basis of successful exploration and discovery of porphyry deposits in the circum-Pacific metallogenic belt (Fig. 1a; e.g., Mitchell and Garson, 1972; Jorhan et al., 1983; Bektas et al., 1990; Solomon, 1990; Rui et al., 2004). More recent discoveries have highlighted the occurrence and formation of porphyry Cu (–Mo–Au) deposits in continent–continent collisional settings, such as in southern Tibet, Iran, and western Pakistan (e.g., Rui et al., 1984; Hou et al., 2001, 2003, 2004, 2009, 2011; Qu et al., 2001; Richards, 2009, 2011a, b; Shafiei et al., 2009; Pettke et al., 2010; Richards et al., 2012; Ayati et al., 2013; Asadi et al., 2014; Fig. 1a, b). Research on deposits in these collisional environments has led to the establishment of a model of collisional orogenic porphyry mineralization (e.g., Rui et al., 2006; Hou et al., 2007, 2009, 2011; Hou and Cook, 2009; Lu et al., 2013; Yang et al., 2014; Wang et al., 2014a, b). The development of porphyry Cu deposits in different tectonic settings, such as those of subduction-related continental margin–arcs (referred to as ‘subduction-related porphyry Cu deposits’ in this study) and continent–continent collisional (referred to as ‘collision-related porphyry Cu deposits’ in this study) settings, suggests that the magmas associated with these deposits were derived either from sources with different compositions and/or formed through different mechanisms.

Although a few studies have compared subduction- and collision-related porphyry Cu deposits (e.g., Hou et al., 2009, 2011), most of this previous research has concentrated on the genetic association between adakitic rocks and porphyry Cu deposits (e.g., Richards and Kerrich,

2007; Richards, 2009; Sun et al., 2011, 2012). Thus, it is unclear whether there are systematic geochemical differences between subduction- and collision-related copper-bearing porphyries. Here, we use published geochemical data for typical patterns of Cu-bearing porphyries to identify differences in geochemical characteristics of subduction- and collision-related Cu-bearing porphyries. The data are from continental margin arc settings along the eastern Pacific Rim (EPRIM; based on two stages of formation, during the Late Cretaceous–Paleogene and the Neogene), and from a continent–continent collision zone in southern Tibet (which formed during the Miocene), and we discuss variations in the source compositions and formation mechanisms of the deposits, thereby providing a basis for further exploration of other areas with tectonic settings suitable for porphyry Cu mineralization.

2 Temporal and spatial distribution of porphyry deposits

Globally, porphyry Cu (–Mo–Au) deposits occur mainly in the circum-Pacific, Tethys–Himalaya, and ancient Asia (Central Asia) metallogenic belts (e.g., Cooke et al., 2005; Sinclair, 2007; Richards, 2013; Sun et al., 2014). The circum-Pacific and Tethys–Himalaya belts formed mainly in the Mesozoic and Cenozoic, and, relatively complete geological data have allowed research into the mechanisms and processes involved in porphyry mineralization. Approximately 97% of large to giant porphyry Cu deposits have formed in magmatic arc settings (e.g., Kerrich et al., 2000; Cooke et al., 2005; Sillitoe, 2010), including the classic metallogenic provinces in island arc settings, such as those of the western Pacific in Indonesia and the Philippines (e.g., Hedenquist and Richards, 1998; Cooke et al., 2005). However, metallogenic porphyry Cu provinces in continental margin–arc environments are generally located in the eastern Pacific, including in the Chile–Peru, Panama–Colombia, southwestern United States–Mexico, and western United States–Canada metallogenic provinces (e.g., Sillitoe, 2010). Large porphyry Cu deposits of the Pacific Rim, which are generally located in the eastern Pacific, developed in the late Mesozoic and Cenozoic (e.g., Cooke et al., 2005). Here, we focus on geochemical data for Cu-bearing porphyries associated with the subduction of oceanic crust that formed during two major phases of metallogenesis in the eastern Pacific. The first phase, in the Late Cretaceous–Paleogene, was associated with the formation of the Laramide porphyry province in Arizona (e.g., Lang and Titley, 1998), the Mezcala porphyry province in Mexico (e.g.,

González-Partida et al., 2003), the El Salvador deposit in the Chilean Porphyry Cu belt (e.g., Baldwin and Pearce, 1982), and the Bingham mining district in Utah (e.g., Stavast et al., 2006). The second phase of metallogenesis occurred during the Miocene, and was associated with the formation of the Bajo de la Alumbrera porphyry Cu-Au deposit in Argentina (e.g., Müller and Forrestal, 1998; Ulrich and Heinrich, 2001), the giant El Teniente Cu-Mo deposit (e.g., Cannell et al., 2005; Stern et al., 2007, 2010; Vry et al., 2010) and the giant Los Pelambres porphyry Cu deposits in central Chile (e.g., Reich et al., 2003), the porphyry Cu-Au deposits of the Refugio District in northern Chile (e.g., Muntean and Einaudi, 2000), and porphyry Cu-Mo deposits in Ecuador (e.g., Chiaradia et al., 2004; Schutte et al., 2010; Fig. 1a).

The majority of the porphyry Cu mineralization in continent–continent collisional settings is located in the central and eastern part of the Tethys–Himalaya metallogenic belt, including the Cenozoic Sungun-Dalli-Sar cheshmeh porphyry Cu belts in Iran, the Gangdese and Yulong porphyry Cu belts in southern and eastern Tibet, respectively. The Cenozoic Sungun-Dalli-Sar cheshmeh porphyry Cu belt mainly occurred during Miocene times (e.g., Shafiei et al., 2009; Haschke et al., 2010; Richards et al., 2012; Ayati et al., 2013; Asadi et al., 2014; Richards, 2014). The Yulong porphyry Cu belt formed during 40 – 35 Ma (e.g., Rui et al., 1984; Ma, 1990; Tang and Luo, 1995; Hou et al., 2006, 2009, 2011; Yang et al., 2009, 2014; Lu et al., 2013), and the Gangdese porphyry Cu belt is an E–W trending ~350 km-long belt located in the Indo-Asian collisional zone and that contains several large and a series of intermediate to small porphyry Cu deposits (e.g., Hou et al., 2004, 2009, 2011; Qu et al., 2004; Wang et al., 2014a, b; Fig. 1b). The majority of fault-controlled porphyry Cu mineralization in the Gangdese belt is hosted in graben controlled by N–S faults (e.g., Hou et al., 2004, 2009, 2011) and formed between 19.7 and 11.5 Ma (e.g., Hou et al., 2003, 2004, 2009, 2011; Qu et al., 2003, 2007, 2009; Rui et al., 2004). These deposits formed as a result of the 65–55 Ma collision between India and Eurasia (e.g., Mo et al., 2007, 2008) and as such developed in a typical continent–continent collision setting. The majority of geochemical data for collision-related porphyry Cu mineralization are from the Gangdese porphyry Cu belt in southern Tibet (Fig. 1b; e.g., Hou et al., 2004; Qu et al., 2004; Guo et al., 2007; Gao et al., 2007a; Wang et al., 2014a, b).

3 Geochemistry

Data was gathered from a variety of studies on ore-bearing porphyry rocks which are mainly from eastern Pacific Rim (EPRIM) and Gangdese belt in southern Tibet, because their geodynamic settings is well constrained. Several data filters were employed to ensure inclusion of only the highest quality data in this study. Samples not meeting the following criteria were excluded from discussion: (1) whole rock SiO_2 concentrations of less than 56 wt.% or greater than 75 wt.%; (2) sample suggested in article texts to be substantially altered, or crustal contamination, or assimilation; (3) data published before or in 1980; (4) major elements plus loss on ignition totals greater than 102% or less than 98 wt.%; (5) total volatile content greater than 3 wt.%.

3.1 Major and trace element geochemistry

Porphyry Cu mineralization on the EPRIM is divided into deposits that formed during the Late Cretaceous–Paleogene (herein CPEPR) and deposits that formed during the Miocene (herein MPEPR). The CPEPR deposits are generally associated with diorite, granodiorite, quartz diorite, quartz monzonites, and granite (e.g., Baldwin and Pearce, 1982; Lang and Titley, 1998; González-Partida et al., 2003). In contrast, the majority of the MPEPR deposits are associated with andesite, monzodiorite, granodiorite, quartz diorites, monzonite and dacite (e.g., Müller and Forrester, 1998; Reich et al., 2003; Cannell et al., 2005; Schutte et al., 2010; Stern et al., 2010; Vry et al., 2010). Miocene porphyry Cu deposits in the continent–continent collisional setting of the Gangdese porphyry Cu belt in southern Tibet (herein MPST) are associated with diorite, granodiorite, quartz monzonite, dacite, monzonitic granite and granite (e.g., Hou et al., 2004; Wang et al., 2014b). The majority of the MPEPR samples are classified as calc-alkaline in K_2O vs. SiO_2 diagram (Fig. 2a), with some high-K calc-alkaline and tholeiitic samples and a small number of alkaline samples. In comparison, the majority of the CPEPR samples (Fig. 2a) are classified as high-K calc-alkaline, with minor calc-alkaline samples. The MPST samples (Fig. 2b) are generally high-K calc-alkaline, with some samples classified as calc-alkaline and alkaline series.

In Harker diagrams (Fig. 3), Al_2O_3 , CaO , Fe_2O_3 , TiO_2 , and MgO concentrations of Cu-bearing porphyries are negatively correlated with SiO_2 concentrations, whereas no clear correlations are observed between Na_2O and SiO_2 concentrations. Although the P_2O_5 concentrations of MPST and CPEPR are negatively correlated with SiO_2 , those of MPEPR have not see this trend (Fig. 3f). In the majority of the porphyries discussed here, $\text{Mg}\#$ values

($Mg\# = 100 \times Mg^{2+} / (Fe^{2+} + Mg^{2+})$) are relatively high (≥ 40), and K_2O concentrations and K_2O/Na_2O ratios are generally higher in collision-related porphyry samples than in subduction-related porphyry samples (Table 1).

Variations in trace element vs. SiO_2 concentrations (Fig. 4) indicate that Sr concentrations are negatively correlated with SiO_2 concentrations in MPST and CPEPR, whereas Th and Zr concentrations in MPST and MPEPR samples show no correlation SiO_2 . All samples from the EPRIM and southern Tibet show similar ranges of concentrations of trace elements (e.g., Zr, Ba, and Sr), although Th concentrations are much higher in the MPST samples than in the EPRIM samples (Fig. 4). Moreover, the Th concentrations of most samples in MPST and some of CPEPR are higher than those of the upper and lower crust (Fig. 4d).

Chondrite-normalized rare earth element (REE) patterns (Fig. 5a–c) indicate clear fractionation between light REEs (LREE) and heavy REEs (HREE) with the latter generally showing flat patterns, and with no significant negative Eu anomalies; the CPEPR and MPST samples show higher LREE concentrations than do the MPEPR samples.

Primitive-mantle-normalized multi-element variation diagrams (Fig. 5d–f) indicate that all samples are significantly enriched in the large ion lithophile elements (LILE; e.g., Rb and U) relative to the high field strength elements (HFSE), and have pronounced negative Nb–Ta–Ti anomalies, with the vast majority of samples also having negative P anomalies. The majority of the MPST samples exhibit HREE concentrations lower than those of the EPRIM samples, and also exhibit negative Ba anomalies. In addition, trace element concentrations in the MPEPR samples are more variable than those in the CPEPR and MPST samples.

3.2 Sr–Nd isotope geochemistry

The MPEPR samples exhibit higher $\epsilon Nd_{(t)}$ values (–2.18 to 6.79) and lower $^{87}Sr/^{86}Sr_{(i)}$ ratios (0.7037–0.7071) than the CPEPR samples ($\epsilon Nd_{(t)}$ of –12.1 to –3.19; $^{87}Sr/^{86}Sr_{(i)}$ of 0.7054–0.7145) (Fig. 6; Table 1). Meanwhile, MPST samples exhibit a wide range of $\epsilon Nd_{(t)}$ (–6.83 to 5.70) and $^{87}Sr/^{86}Sr_{(i)}$ (0.7034–0.7091) isotope ratios (Table 1; Fig. 6). All of the samples plot between Mid-Ocean Ridge Basalt (MORB) and mantle-derived ultrapotassic rocks on a Sr vs. Nd isotope diagram (Fig. 6).

3.3 Adakitic characteristics of Cu-bearing porphyry intrusions

Adakites formed from magmas generated by partial melting of a subducted slab in the garnet stability field (Defant and Drummond, 1990; Defant et al., 1992). These rocks have high concentrations of SiO_2 (>56 wt.%) and Al_2O_3 (>15 wt.%), low concentrations of MgO (<3 wt.%), Y, and HREE (Y and Yb concentrations of <18 and <1.9 ppm, respectively), high LILE concentrations, and Sr concentrations of >400 ppm. Those rocks with adakite-like compositions is referred to as adakitic rocks (e.g., Chung et al., 2003; Hou et al., 2004; Castillo, 2012), which can be produced by assimilation and fractional crystallization (AFC), the melting of delaminated lower crust, partial melting of the lower crust and other model. It is an intense debate topic whether there is a link between adakitic magmas and porphyry mineralization in continental margin–arc and post-subduction settings (e.g., Thiéblemont et al., 1997; Sajona and Maury, 1998; Oyarzun et al., 2001, 2002; Rabbia et al., 2002; Richards, 2002, 2009, 2011a, b; Richards and Kerrich, 2007; Wang et al., 2008; Castillo, 2012; Sun et al., 2011, 2012). Nevertheless, all of the MPST samples are classified as adakitic rocks in the Sr/Y vs. Y (Fig. 7a, b) and $(\text{La}/\text{Yb})_N$ vs. $(\text{La})_N$ diagrams (Fig. 7c, d) that are typically used to distinguish adakitic rocks from normal arc andesites, dacites, and rhyolites (ADR). In comparison, some of the EPRIM samples are classified as adakitic rocks, with the rest plotting in the ADR field. The published data for Cu-bearing porphyries on the EPRIM and in southern Tibet indicate that the former have generally higher Y concentrations and lower Sr/Y and $(\text{La}/\text{Yb})_N$ values than the latter (Table 1), indicating a temporal–spatial relationship between adakitic rocks and porphyry Cu deposits in the EPRIM and southern Tibet (e.g., Thiéblemont et al., 1997; Sajona and Maury, 1998; Defant and Kepezhinskas, 2001; Oyarzun et al., 2001, Mungall, 2002; Hou et al., 2004), although not all mineralized porphyries are adakitic (e.g., Hou et al., 2011).

4 Discussion

4.1 Origin of porphyry Cu deposits in collisional orogenic settings

Porphyry Cu deposits that formed in continental arc settings, such as the porphyry Cu mineralization on the EPRIM, have been intensively studied (e.g., Sillitoe, 1972; Richards, 2003, 2009, 2011a, b, 2013; Cooke et al., 2005). However, the processes involved in the formation of porphyry Cu deposits in collisional orogenic settings remain, and these processes are considered in

this section.

The formation of porphyry Cu mineralization is associated with high oxygen-fugacity (fO_2) magmas that contain high concentrations of H_2O and Cu (Sillitoe, 1997; Parkinson and Arculus, 1999; Mungall, 2002; Sun et al., 2004, 2010, 2012, 2013; Hou et al., 2009, 2011; Richards, 2009, 2011a, b). A certain high- fO_2 conditions can cause Cu concentrations to increase in the magma at the sulphide-sulphate transition, thus promoting mineralization (e.g., Ballard et al., 2002; Mungall, 2002; Richards, 2003; Sillitoe, 2010; Botcharnikov et al., 2011). In comparison, high H_2O concentrations are essential to the efficient removal of ore metals from silicate melts during emplacement in the upper crust (e.g., Burnham, 1979; Richards, 2009; Richards et al., 2012). Furthermore, arc basalts and MORB have higher Cu concentrations than the continental crust, the lower continental crust, and the primitive upper mantle (e.g., Sun, 1982; Rudnick and Gao, 2003; Sun et al., 2011, 2013). Consequently, porphyry Cu deposits are generally thought to form from hydrothermal fluids exsolved from hydrous, high- fO_2 , sulfur-rich arc magmas derived from a metasomatized mantle wedge that formed during slab subduction (e.g., Arculus, 1994; Noll et al., 1996; De Hoog et al., 2001; McInnes et al., 2001; Sun et al., 2003, 2004, 2013; Mungall et al., 2006; Richards, 2009, 2011a, b; Wallace and Edmonds, 2011).

It is thought that the crust beneath southern Tibet is twice as thick as the thickness of normal crust as a result of collision between the Asian and Indian plates (e.g., Zhao and Nelson, 1993; Owens and Zandt, 1997). However, extensive Andean-type calc-alkaline magmatism in the southern part of the Lhasa Terrane (Linzizong volcanics and Gangdese batholiths, ~195 to 45 Ma; e.g., Mo et al., 2007, 2008; Chung et al., 2009; Kang et al., 2014) involved magmas derived from a metasomatized mantle wedge with normal crustal thickness (30–40 km; Chung et al., 2003, 2009). The whole rock geochemistry, Sr–Nd isotope compositions, and zircon Hf isotopic data of ~38–9 Ma adakitic rocks in southern Tibet suggest that the crust in this area underwent a major phase of tectonic thickening (by up to 50 km) between ~45 and 30 Ma (e.g., Chung et al., 2003, 2009; Hou et al., 2004; Guan et al., 2012; Zheng et al., 2012) that was not caused by the impingement of Indian continental crust (e.g., Chung et al., 2009; Hou et al., 2009, 2011; Zheng et al., 2012). This finding, combined with the absence of significant folding in the Tertiary Linzizong volcanics, suggests that the crustal thickening in southern Tibet resulted from large-scale underplating of mantle-derived basaltic magmas (e.g., Mo et al., 2007, 2008; Chung et al., 2009;

Hou et al., 2009; Zheng et al., 2012), rather than from shortening of the upper crust (e.g., Tapponnier et al., 2001).

Miocene porphyry Cu deposits are located in the southern Lhasa subterrane (Fig. 1b), a section of juvenile crust associated with the Late Triassic to early Tertiary 220–40 Ma subduction and accretionary of Tethyan Ocean crust (e.g., Mo et al., 2007, 2008; Chung et al., 2009; Ji et al., 2009; Zhu et al., 2009, 2011). In addition, the fact that the volcanism that formed the Paleogene Linzizong volcanics only occurred in the southern part of the Lhasa Terrane is thought to be a result of breakoff of the subducted Neotethyan slab (e.g., Chung et al., 2009; Lee et al., 2009). The Miocene MPST porphyries that host Cu mineralization exhibit lower Nd and higher Sr isotope ratios than MORB (Fig. 6), similar to the Linzizong volcanics (e.g., Mo et al., 2007; Chung et al., 2009; Chen et al., 2011). This result, combined with the regional evolution of southern Tibet during the Cenozoic and the fact that the Miocene MPST porphyries have adakitic compositional affinities and were sourced from a thickened region of the lower crust (e.g., Chung et al., 2003, 2005, 2009; Hou et al., 2004), suggests that Miocene collisional orogenic porphyry Cu mineralization in southern Tibet formed as a result of the following: slab-breakoff of the northward-subducting Neotethyan oceanic lithosphere from Indian continental lithosphere at ac. ~50 Ma in the early stage of the India-Asia collision (e.g., Chung et al., 2003, 2009; Lee et al., 2009) induced partial melting of metasomatised mantle wedge material that had interacted with fluids and subducted sediment melts, including slab-derived melts generated during and after the breakoff. These high- fO_2 arc-like basaltic melts contained elevated concentrations of chalcophile elements (such as Cu) and volatiles (such as H_2O and Cl), and they ascended and underplated the lower crust in southern Tibet after the termination of Gangdese/Linzizong magmatism and generation of an orogenic root created (~45–30 Ma; e.g., Chung et al., 2003, 2009). Unlike in continental arc settings, these underplated basaltic magmas probably did not mainly undergo a process of melting, assimilation, storage, and homogenization (MASH) to form volatile-rich, high- fO_2 , Cu-bearing intermediate–felsic magmas (e.g., Hou and Cook, 2009; Hou et al., 2009, 2011). Instead, these underplated magmas gradually cooled and transformed to amphibolites and eclogitic amphibolites, and crustal thickness increased (e.g., Chung et al., 2003, 2009; Hou et al., 2004, 2009, 2011) during continuous N–S compression associated with India–Asia continental collision.

Widespread 24–12 Ma magmatism and the formation of 24–10 Ma porphyry Cu mineralization in N–S graben in southern Tibet suggests that this area underwent a transition from tectonic compression to extension during the Miocene (e.g., Coleman and Hodges, 1995; Blisniuk et al., 2001; Williams et al., 2001; Spicer et al., 2003; Hou et al., 2004; Guo et al., 2007). Either this regional tectonic regime, the breakoff of northward-subducting Indian lithosphere (e.g., Mahéo et al., 2002; Williams et al., 2004; Wang et al., 2014a, b), or the foundering/delamination/convective removal of thickening subcontinental lithospheric mantle beneath southern Tibet (e.g., Turner et al., 1993, 1996; Chung et al., 2009; Zhao et al., 2009) caused the asthenospheric mantle beneath southern Tibet to ascend. This rising asthenosphere caused not only the formation of widespread N–S striking extension faults (e.g., Coleman and Hodges 1995; Blisniuk et al., 2001; Williams et al., 2001), but also partial melting of a region of enriched mantle (e.g., Turner et al., 1996; Miller et al., 1999; Williams et al., 2004; Zhao et al., 2009), generating parental magmas that formed ultrapotassic and potassic rocks in southern Tibet. The high geothermal gradient in the area (e.g., Liu et al., 2011), along with decompression associated with E–W extension, underplating, and the uprising of hot mantle-derived magmas, triggered partial melting of the newly formed Cu-bearing amphibolite or eclogitic amphibolite lower crust, generating adakitic melts in southern Tibet. Considered the relatively water poor amphibole–eclogite or garnet–amphibolite in collisional orogens (average estimated maximum H₂O contents: 1.2 wt.%; Leech, 2001) is not efficiently produce adakitic melts having the high H₂O contents (>5 wt.%) of the porphyry Cu–Mo (–Au) ore-forming magma (Wolf and Wyllie, 1991; Skjerlie and Patino Douce, 2002; Yang et al., 2014), the mantle-derived potassic and ultrapotassic magmas that contained abundant volatiles (e.g., H₂O and Cl) (e.g., Rock, 1987; Rock et al., 1990; Foley et al., 1992; Behrens et al., 2009) probably mixed with high-*f*O₂ crustal-derived adakitic melts that contained high concentrations of chalcophile elements (such as Cu), H₂O, and other volatile components released during the partial melting of amphibolite, before these mixed magmas ascended into the upper crust along extensional structures and structural weaknesses, most likely producing Cu-bearing porphyries in southern Tibet.

4.2 Potassium-rich characteristics of mineralized Cu porphyries

The high K₂O and some LILEs (e.g., Ba and Rb) concentrations in the porphyry can be

related to the potassic alteration and/or crustal assimilation. However, the low loss on ignition ($\text{LOI} \leq 3 \text{ wt.}\%$) of samples in this study suggests that the potassic alteration is not important. Meanwhile, obviously higher K_2O , Rb, and Ba concentrations of most samples than the upper continental crust (Figs. 4a, 8a, b, c), combined with the relationship between Mg# and K_2O , Rb, and Ba (Figs. 4a, 8a, b, c), is inconsistent with the crustal assimilation. In addition, the high Ce/Yb ratios (>20) of most ore-bearing porphyries in this study can represent their primary magma (Müller and Forrestal, 2000; Fig. 8d). Therefore, the intermediate to felsic calc-alkaline mineralized Cu porphyries contain elevated concentrations of K as compared with normal arc magmas (e.g., Richards, 2009), and are commonly closely related to alkalic or potassic magmas (e.g., Sillitoe, 1991, 1997, 2002; Sillitoe and Camus, 1991; Vila and Sillitoe, 1991; Barrie, 1993; Kirkham and Margolis, 1995; Lang et al., 1995; Kirkham and Sinclair, 1996; Keith et al., 1997; Müller and Forrestal, 1998; Holliday et al., 2002; Yang et al., 2014; Fig. 1). In addition, Sillitoe (2002) considered that some porphyry Cu-Au deposits are related to alkalic magmatism in arc terranes; and Müller and Groves (1993) suggested that the presence of potassic rocks could be used as an exploration tool and may suggest that an area is highly prospective for porphyry Cu-Au deposits. The majority of samples discussed here have high Mg# values (>40 ; Fig. 3h), suggesting that magmas associated with porphyry Cu deposits contain mantle-derived components (Rapp and Watson, 1995). For example, the high-grade Bingham porphyry Cu (-Mo-Au) deposit on the EPRIM is the product of mixing between an evolving magmatic system and injections of mafic alkaline magmas (e.g., Keith et al., 1997; Hattori and Keith, 2001; Maughan et al., 2002; Pettke et al., 2010). In addition, the presence of porphyry mineralization and both alkalic and adakitic rocks in post-collisional settings are considered to be related with mafic alkalic magmatism (e.g., Richards, 1995; Shafiei et al., 2009; Yang et al., 2014). Furthermore, the essential H_2O contents of porphyry Cu ore-forming magmas ($>5 \text{ wt.}\%$; Wolf and Wyllie, 1991; Skjerlie and Patino Douce, 2002) developed in post-collisional settings cannot be satisfied by only partial melting amphibolite or eclogite (Leech, 2001) as above discussion and need additional water (Yang et al., 2014). Therefore, the Miocene Cu-bearing porphyry in southern Tibet involves both alkaline and high-K calc-alkaline series magmatism (e.g., Hou et al., 2004, 2009, 2011; Fig. 2b) and is thought to have resulted from the mixing of lower-crust-derived melts and mantle-derived potassic-ultrapotassic magmas (e.g., Guo et al., 2007).

Although ultrapotassic rocks are widespread globally and are related to some porphyry deposits (Fig. 1), the majority of samples in this study (with the exception of a few ultrapotassic samples in the Bingham district; Maughan et al., 2002), including limited data for Miocene ultrapotassic rocks of the EPRI (Kay et al., 1994; Redwood and Rice, 1997; Sandeman and Clark, 2004; Maria and Luhe, 2008; Gómez-Tuena et al., 2011) and southern Tibet (Miller et al., 1999; Ding et al., 2003, 2006; Williams et al., 2004; Gao et al., 2007b; Zhao et al., 2009; Chen et al., 2012), do not contain high concentrations of Cu (<130 ppm). However, these mantle-derived potassic and ultrapotassic magmas are typically enriched in the LILE, LREE, and volatiles such as H₂O, CO₂, F, and Cl (e.g., Rock, 1987; Rock et al., 1990; Behrens et al., 2009), all of which likely enhance the solubility of chalcophile elements, such as Cu and Au, in high-temperature aqueous fluids (e.g., Heinrich et al., 1992; Pokrovski et al., 2005, 2008; Simon et al., 2005, 2006; Zajacz et al., 2008, 2011; Seo et al., 2009). This indicates that the generally high K₂O concentrations (K₂O/Na₂O > 0.5) in magmas associated with porphyry Cu mineralization are most likely produced by mixing between melts derived from the underplated basaltic lower crust and ascending mantle-derived potassic and ultrapotassic magmas (e.g., Pettke et al., 2010; Yang et al., 2014). This interpretation is consistent with the Sr–Nd isotope compositions of the samples discussed here, all of which plot between MORB and ultrapotassic magma compositions in a Sr vs. Nd isotope diagram (Fig. 6).

4.3 Comparison of between subduction- and collision-related Cu porphyries

As discussed above, the formation of subduction- and collision-related porphyry Cu ore-forming magmas derived from sources with different processes and/or compositions. Here, we use the geochemical data described above to compare subduction- and collision-related porphyry Cu mineralization.

4.3.1 Similarities

4.3.1.1. Components related to arc magmatism

Although the arc magmatism is clearly linked to the development of porphyry Cu deposits on the EPRI in spatial, the geochemistry of Cu porphyries in collisional zones, such as LILE enrichment (e.g., Rb, K, Th, U and Sr), HFSE depletion (e.g., Nb, Ta and Ti), and depletions in

HREE and Y, are also similar to those observed in typical subduction-related magmas (Fig. 5d–f; e.g., Wilson, 1989), suggesting that these subduction signature in collision-related porphyries is probably resulted from the reactivation of subduction-modified material of arc magma before continental collisions (e.g., Hou et al., 2004, 2009, 2011; Richards et al., 2009, 2011a, b).

4.3.1.2. Thickened crust

Recent studies indicate that porphyry Cu deposits are located in thick mature continental arcs (e.g., Cook et al., 2005; Sillitoe, 2010; Lee et al., 2012) and collisional orogenic belts (e.g., Hou et al., 2004, 2009, 2011; Yang et al., 2014). Compressional tectonics, caused by the subduction of oceanic crust or continent–continent collision, lead to localized deformation and crustal thickening immediately prior to emplacement of mineralized intrusions in continental arc settings (e.g., Sillitoe, 1998; Kay et al., 1999) and orogenic collisional zones (e.g., Hou et al., 2009, 2011). This thickening of the crust favors MASH-type underplating of primitive metasomatized mantle-wedge-derived magmas beneath the lower crust. This process can yield evolved, volatile-rich, metalliferous hybrid intermediate (andesitic–dacitic) melts (e.g., Richards, 2003; Hou et al., 2009; Wang et al., 2014b). By comparison, thickened crust (>50–45 km) can cause the underplated basaltic material to transform to amphibolites and eclogitic amphibolites (e.g., Defant and Drummond, 1990; Rapp et al., 1999), thus affecting the concentration of water in the magma. Contrast to the mass water carried by the subducted oceanic slab in the continental arc, the water content for porphyry Cu (Mo–Au) formation in the collisional settings is likely storage in amphibole-bearing mineral assemblages that were stable during earlier stages of crustal thickening and break down to release water during late stage magma activity (Kay and Mpodozis, 2001; Richards, 2009).

4.3.2 Differences

4.3.2.1. Depth of generation of Cu-bearing porphyry magmas

Thickened regions of the crust are characteristically associated with porphyry Cu deposits, as discussed above. However, most samples of MPST exhibit higher $(La/Yb)_N$ (11.7–63.0, average of 31.1) ratios than do MPEPR (1.67–53.1, average of 13.0) and CPEPR (7.95–34.7, average of 18.6) samples (Table 1; Figs. 5, 7), implying that the MPST samples formed from magmas sourced

deeper than those associated with the EPRIM samples (e.g., Haschke et al., 2002; Haschke and Günther, 2003; Chung et al., 2009). The magma source depths of MPST is probably related with the underplated mafic magmas and increasing crustal thickness during Eocene and Oligocene (e.g., Chung et al., 2009). In contrast, the formation of MPEPR are related with the shallowing subduction zone or during the initial steepening of a formerly flat subduction zone (Kay and Mpodozis, 2001). In addition, some EPRIM samples are exhibit high La/Yb values, which probably caused by residual garnet in their source and formed in a mature continental arc setting (Müller and Forrester, 1998).

4.3.2.2. Enrichment mechanisms

Porphyry Cu mineralization is associated with magmas that contain abundant fluids (e.g., H₂O) and other volatile components (e.g., Cl and F), suggesting that these magmas underwent some sort of enrichment process. Although some LILEs (e.g., Rb, and Ba) and Th concentrations can be caused by the crustal contamination, the obviously higher Rb, Ba, and Th concentrations of most samples in this study than the upper continental crust imply that the crustal assimilation is not important as above discussion (Figs. 4, 8). So, the differences in LILE (such as Ba) and HFSE (such as Th) abundances and LILE/HFSE ratios (such as Ba/Yb, Sr/Yb, Nb/Yb, and Th/Yb) between porphyry Cu mineralization in southern Tibet and on the EPRIM suggest that the former have been enriched by interactions with melts, whereas the latter have been enriched by interaction with fluids (Fig. 9a, b, c). This inference is consistent with the formation of these deposits in different tectonic regimes (continent–continent collision and continental margin–arc settings, respectively) and different formation processes, as discussed above.

Two different evolutionary trends of samples from southern Tibet and the EPRIM are evident in a Th/La vs. Sm/La diagram (Fig. 9d). Tommasini et al. (2011) suggested that significantly high Th concentrations in mantle-derived ultrapotassic magmas are associated with components derived from a high Sm/La and Th/La source. In addition, the high Th/La values of porphyry Cu mineralization in southern Tibet, which are similar to those of coexisting ultrapotassic magmas, combined with similar to variable high Th/Yb and Nb/Y trends in both magmas, and the presence of newly formed crust in southern Tibet (as discussed above), suggest a link between porphyry Cu mineralization and coexisting Miocene potassic and ultrapotassic magmas in southern Tibet as above discussion.

5 Conclusions

1. Porphyry Cu (–Mo–Au) deposits occur not only in continental margin settings (such as the EPRIM) but also in continent–continent collisional orogenic belts (such as southern Tibet). These deposits developed in different tectonic regimes and show some differences in some trace element (e.g., Th, and Y) concentrations and ratios (e.g., Sr/Y, and La/Yb), implying that they underwent different formation processes and/or were derived from sources with different compositions.

2. Subduction-related porphyry Cu mineralization is probably associated with magmas generated by underplated mafic material that underwent a MASH process, whereas collision-related porphyry Cu mineralization is produced by a process in which underplated arc-like basaltic magma beneath the lower crust is gradually cooling and transformed into amphibolites and eclogitic amphibolites, which then undergo partial melting and interaction with underplated potassic and ultrapotassic melts from an enriched mantle. These differences in the formation processes cause some differences in geochemistry, such as the adakitic affinity and melt-enriched compositions recorded in collision-related Cu porphyries, and the contrasting evolution of subduction-related Cu porphyries which record an evolution from normal arc rocks to adakitic rocks, and which are characterized by fluid-dominated enrichment.

3. Magmas associated with both subduction- and collision-related porphyry Cu mineralization are generated during crustal thickening and compressional tectonism. In addition, their high K₂O contents are probably derived from (1) the inheritance of enriched mantle components and/or (2) mixing with contemporary mantle-derived ultrapotassic magmas.

Acknowledgements

We are grateful to the Chief Editor Franco Pirajno, the Guest Editor Zeng-Qian Hou, and two anonymous reviewers for their kind and critically constructive comments and suggestions, which greatly improved the quality of our manuscript. This research was supported by the following funding agencies: the Major State Basic Research Program of the People's Republic of China (2015CB452602, 2011CB403100), the Strategic Priority Research Program (B) of the Chinese Academy of Sciences (XDB03010300), the Natural Science Foundation of China (41373030), the

IGCP project (IGCP/SIDA-600), and the GIGCAS 135 project of the Guangzhou Institute of Geochemistry (Y2340202),. This is GIGCAS contribution No. IS-XXX.

ACCEPTED MANUSCRIPT

References

- Arculus, R.J., 1994. Aspects of magma genesis in arcs. *Lithos* 33, 189–208.
- Asadi, S., Moore, F., Zarasvandi, A., 2014. Discriminating productive and barren porphyry copper deposits in the southeastern part of the central Iranian volcano-plutonic belt, Kerman region, Iran: A review. *Earth-Science Reviews* 138, 25–46.
- Ayati, F., Yavuz, F., Asadi, H.H., Richards, J.P., Jourdan, F., 2013. Petrology and geochemistry of calc-alkaline volcanic and subvolcanic rocks, Dalli porphyry copper–gold deposit, Markazi Province, Iran. *International Geology Review* 55, 158–184.
- Baldwin, J.A., Pearce, J.A., 1982. Discrimination of productive and nonproductive porphyritic intrusions in the Chilean Andes. *Economic Geology* 77, 664–674.
- Ballard, J.R., Palin, J.M., Campbell, I.H., 2002. Relative oxidation states of magmas inferred from Ce(IV)/Ce(III) in zircon: application to porphyry copper deposits of northern Chile. *Contribution to Mineralogy and Petrology* 144, 347–364.
- Barrie, C.T., 1993. Petrochemistry of shoshonitic rocks associated with porphyry-gold deposits of central Quesnellia, British Columbia, Canada. *Journal of Geochemical Exploration* 48, 225–258.
- Behrens, H., Misiti, V., Freda, C., Vetere, F., Botcharnikov, R.E., Scarlato, P., 2009. Solubility of H₂O and CO₂ in ultrapotassic melts at 1200 and 1250°C and pressure from 50 to 500 MPa. *American Mineralogist* 94, 105–120.
- Bektas, O., Vassileff, L., Stanisheva, V.G., 1990. Porphyry copper systems as markers of the Mesozoic-Cenozoic active margin of Eurasia: discussion and reply. *Tectonophysics* 172, 191–194.
- Blisniuk, P.M., Hacker, B., Glodny, J., Ratschbacher, L., Bil, S., Wu, Z.H., McWilliams, M.O., Calvert, A., 2001. Normal faulting in central Tibet since at least 13.5 Myr ago. *Nature* 412, 628–632.
- Botcharnikov, R.E., Linnen, R.L., Holtz, W.M., Jugo, P.J., Berndt, J., 2011. High gold concentrations in sulphide-bearing magma under oxidizing conditions. *Nature Geoscience* 4, 112–115.
- Burnham, C.W., 1979. Magmas and hydrothermal fluids. In: Barnes HL (ed.) *Geochemistry of Hydrothermal Ore Deposits*, 2nd Edition. New York: Wiley. 71–136.
- Cannell, J., Cooker, D.R., Walshe, J.L., Stein, H., 2005. Geology, mineralization, alteration, and structural evolution of the El Teniente porphyry Cu-Mo deposit. *Economic Geology* 100, 979–1003.
- Carlier, G., Lorand, J.P., 2003. Petrogenesis of a zirconolite-bearing Mediterranean-type lamproite from the Peruvian Altiplano (Andean Cordillera). *Lithos* 69, 15–35.
- Carlier, G., Lorand, J.P., Audebaud, E., Kienast, J.R., 1997. Petrology of an unusual orthophoxene-bearing minette suite from southeastern Peru, Eastern Andean Cordillera: Al-rich lamproites contaminated by peraluminous granites. *Journal of Volcanology and Geothermal Research* 75, 59–87.
- Castillo, P.R., 2012. Adakite petrogenesis. *Lithos* 134–135, 304–316.
- Chen, J.L., Xu, J.F., Wang, B.D., Kang, Z.Q., 2012. Cenozoic Mg-rich potassic rocks in the Tibetan Plateau: geochemical variations, heterogeneity of subcontinental lithospheric mantle and tectonic implications. *Journal of Asian Earth Sciences* 53, 115–130.

- Chen, J.L., Xu, J.F., Zhao, W.X., Dong, Y.H., Wang, B.D., Kang, Z.Q., 2011. Geochemical variations in Miocene adakitic rocks from the western and eastern Lhasa terrane: implications for lower crustal flow beneath the southern Tibetan plateau. *Lithos* 125, 928–939.
- Chiaradia, M., Fontboté, L., Beate, B., 2004. Cenozoic continental arc magmatism and associated mineralization in Ecuador. *Mineralium Deposita* 39, 204–222.
- Chung, S.L., Chu, M.F., Ji, J.Q., O'Reilly, S.Y., Person, N.J., Liu, D.Y., Lee, T.Y., Lo, C.H., 2009. The nature and timing of crustal thickening in Southern Tibet: Geochemical and zircon Hf isotopic constraints from postcollisional adakites. *Tectonophysics* 477, 36–48.
- Chung, S.L., Chu, M.F., Zhang, Y., Xie, Y., Lo, C.H., Lee, T.Y., Lan, C.Y., Li, X., Zhang, Y.Q., Wang, Y., 2005. Tibetan tectonic evolution inferred from spatial and temporal variations in post-collisional magmatism. *Earth Science Reviews* 68, 173–196.
- Chung, S.L., Liu, D.Y., Ji, J.Q., Lee, H.Y., Wen, D.J., Lo, C.H., Lee, T.Y., Qian, Q., Zhang, Q., 2003. Adakites from continental collision zones: Melting of thickened lower crust beneath southern Tibet. *Geology* 31, 1021–1024.
- Coleman, M., Hodges, K., 1995. Evidence for Tibetan plateau uplift before 14 Myr ago from a new minimum age for east-west extension. *Nature* 374, 49–52.
- Conticelli, S., Carlson, R.W., Widom, E., Serri, G., 2007. Chemical and isotopic composition (Os, Pb, Nd, and Sr) of Neogene to Quaternary calc-alkalic, shoshonitic, and ultrapotassic mafic rocks from the Italian peninsula: inferences on the nature of their mantle sources. *Geological Society of America Special Paper* 418, 171–202.
- Cooke, D.R., Hollings, P., Walshe, J.L., 2005. Giant Porphyry Deposits: Characteristics, distribution, and tectonic controls. *Economic Geology* 100, 801–818.
- De Hoog, J., Mason, P., Van Bergen, M., 2001. Sulfur and chalcophile elements in subduction zones: constraints from a laser ablation ICP-MS study of melt inclusions from Galunggung Volcano, Indonesia. *Geochimica et Cosmochimica Acta* 65, 3147–3164.
- Defant, M.J., Drummond, M.S., 1990. Derivation of some modern arc magmas by melting of young subducted lithosphere. *Nature* 347, 662–665.
- Defant, M.J., Jackson, T.E., Drummond, M.S., de Boer, J.Z., Bellon, H., Feigenson, M.D., Maury, R.C., Stewart, R.H., 1992. The geochemistry of young volcanism throughout western Panama and southeastern Costa Rica: an overview. *Journal of the Geological Society* 149, 569–579.
- Defant, M.J., Kepezhinskas, P., 2001. Adakites: A review of slab melting over the past decade and the case for a slab-melt component in arcs. *EOS, Transactions* 82(65), 68–69.
- Ding, L., Kapp, P., Zhong, D.L., Deng, W.M., 2003. Cenozoic volcanism in Tibet: Evidence for a transition from oceanic to continental subduction. *Journal of Petrology* 44, 1833–1865.
- Ding, L., Yue, Y., Cai, F., Xu, X., Zhang, Q., Lai, Q., 2006. ^{40}Ar - ^{39}Ar geochronology, geochemical and Sr-Nd-Pb isotopic characteristic of the high-Mg ultrapotassic rocks in Lhasa block of Tibet: implications in the onset time and depth of NS-striking rift system. *Acta Geological Sinica* 80, 1252–1261 (in Chinese with English abstract).

- Drummond, M.S., Defant, M.J., 1990. A model for trondhjemite–tonalite–dacite genesis and crustal growth via slab melting: Archean to modern comparisons. *Journal of Geophysical Research* 95, 21503–21521.
- Foley, S., 1992. Petrological characterization of the source components of potassic magmas: geochemical and experimental constraints. *Lithos* 28, 187–204.
- Gao, Y., Hou, Z., Kamber, B.S., Wei, R., Meng, X., Zhao, R., 2007b. Lamproitic rocks from a continental collision zone: evidence for recycling of subduction Tethyan Oceanic sediments in the mantle beneath southern Tibet. *Journal of Petrology* 48, 729–752.
- Gao, Y.F., Hou, Z.Q., Kamber, B.S., Wei, R.H., Meng, X.J., Zhao, R.S., 2007a. Adakite-like porphyries from the southern Tibetan continental collision zones: evidence for slab melt metasomatism. *Contributions to Mineralogy and Petrology* 153, 105–120.
- Gómez-Tuena, A., Mori, L., Goldstein, S.L., Pérez-Arvizu, O., 2011. Magmatic diversity of western Mexico as a function of metamorphic transformations in the subducted oceanic plate. *Geochimica et Cosmochimica Acta* 75, 213–241.
- González-Partida, E., Levrresse, G., Carrillo-Chávez, A., Cheilletz, A., Gasquet, D., Jones, D., 2003. Paleocene adakite Au-Fe bearing rocks, Mezcala, Mexico: evidence from geochemical characteristics. *Journal of Geochemical Exploration* 80, 25–40.
- Guan, Q., Zhu, D.C., Zhao, Z.D., Dong, G.C., Zhang, L.L., Li, X.W., Liu, M., Mo, X.X., Liu, Y.S., Yuan, H.L., 2012. Crustal thickening prior to 38 Ma in southern Tibet: evidence from lower crust-derived adakitic magmatism in the Gangdese Batholith. *Gondwana Research* 21, 88–99.
- Guo, Z.F., Wilson, M., Liu, J.Q., 2007. Post-collisional adakites in south Tibet: Products of partial melting of subduction-modified lower crust. *Lithos* 96, 205–224.
- Haschke, M., Ahmadian, J., Murata, M., McDonald, I., 2010. Copper mineralization prevented by arc-root delamination during Alpine–Himalayan collision in Central Iran. *Economic Geology* 105, 855–865.
- Haschke, M., Günther, A., 2003. Balancing crustal thickening in arcs by tectonic vs. magmatic means. *Geology* 31, 933–936.
- Haschke, M., Siebel, W., Günther, A., Scheuber, E., 2002. Repeated crustal thickening and recycling during the Andean orogeny in north Chile (21°–26°S). *Journal of Geophysical Research* 107, B1, 2019, 10.1029/2001JB000328.
- Hattori, K.H., Keith, J.D., 2001. Contribution of mafic melt to porphyry copper mineralization: evidence from Mount Pinatubo, Philippines, and Bingham deposit, Utah. *Mineralium Deposita* 36, 799–806.
- Hedenquist, J.W., Richards, J.P., 1998. The influence of geochemical techniques on the development of genetic models for porphyry copper deposits. *Reviews in Economic Geology* 10, 235–256.
- Heinrich, C.A., Ryan, G.G., Mernagh, T.P., Eadington, P.J., 1992. Segregation of ore metals between magmatic brine and vapor: a fluid inclusion study using PIXE microanalysis. *Economic Geology* 87, 1566–1583.
- Hofmann, A.W., 2003. Sampling mantle heterogeneity through oceanic basalts; isotopes and trace elements. In: *The mantle and Core, vol.2. Treatise on Geochemistry* (eds. Holland HD and Turekian KK). Elsevier-Pergamon, Oxford 61–101.

- Holliday, J.R., Wilson, A.J., Blevin, P.L., Tedder, I.J., Dunham, P.D., Pfitzner, M., 2002. Porphyry gold-copper mineralization in the Cadia district, eastern Lachlan Fold Belt, New South Wales, and its relationship to shoshonitic magmatism. *Mineralium Deposita* 37, 100–116.
- Hou, Z.Q., Cook, N.J., 2009. Metallogenesis of the Tibetan Collisional Orogen: a review and introduction to the special issue. *Ore Geology Reviews* 36, 2–24.
- Hou, Z.Q., Gao, Y.F., Qu, X.M., Rui, Z.Y., Mo, X.X., 2004. Origin of adakitic intrusives generated during mid-Miocene east-west extension in southern Tibet. *Earth and Planetary Science Letters* 220, 139–155.
- Hou, Z.Q., Ma, H.W., Zaw, K., Zhang, Y.Q., Wang, M.J., Wang, Z., Pan, G.T., Tang, R.L., 2003. The Himalayan Yulong porphyry copper belt: Product of large-scale strike-slip faulting in eastern Tibet. *Economic Geology* 98, 125–145.
- Hou, Z.Q., Qu, X.M., Huang, W., Gao, Y.F., 2001. The Gangdese porphyry copper belt: the second significant porphyry copper belt in Tibetan plateau. *Chinese Geology* 28, 27–30 (in Chinese with English abstract).
- Hou, Z.Q., Yang, Z.M., Pan, X.F., Qu, X.M., 2007. Porphyry Cu–(Mo–Au) deposits no related to oceanic-slab subduction. *Geosciences* 21, 332–351 (in Chinese with English abstract).
- Hou, Z.Q., Yang, Z.M., Qu, X.M., Rui, Z.Y., Meng, X.J., Gao, Y.F., 2009. The Miocene Gangdese porphyry copper belt generated during post-collisional extension in the Tibetan Orogen. *Ore Geology Reviews* 36, 25–51.
- Hou, Z.Q., Zeng, P.S., Gao, Y.F., Dong, F.L., 2006. The Himalayan Cu–Mo–Au mineralization in the eastern Indo-Asian Collision Zone: constraints from Re–Os dating of molybdenite. *Mineralium Deposita* 41, 33–45.
- Hou, Z.Q., Zhang, H.R., Pan, X.F., Yang, Z.M., 2011. Porphyry Cu (-Mo-Au) deposits related to melting of thickened mafic lower crust: examples from the eastern Tethyan metallogenic domain. *Ore Geology Reviews* 39, 21–45.
- Ji, W.Q., Wu, F.Y., Chung, S.L., Li, J.X., Liu, C.Z., 2009. Zircon U–Pb geochronology and Hf isotopic constraints on petrogenesis of the Gangdese batholith, southern Tibet. *Chemical Geology* 262, 229–245.
- Jiménez, N., López-Velásquez, S., 2008. Magmatism in the Huarina belt, Bolivia, and its geotectonic implications. *Tectonophysics* 459, 85–106.
- Jorhan, T.E., Isacks, B.L., Allmendinger, R.W., Brewer, J.A., Ramos, V.A., Ando, C.J., 1983. Andean tectonic related to geometry of subducted Nazca plate. *Geological Society of America Bulletin* 94, 341–361.
- Kang, Z.Q., Xu, J.F., Wilde, S.A., Feng, Z.H., Chen, J.L., Wang, B.D., Fu, W.C., Pan, H.B., 2014. Geochronology and geochemistry of the Sangri Group Volcanic Rocks, Southern Lhasa Terrane: Implications for the early subduction history of the Neo-Tethys and Gangdese Magmatic Arc. *Lithos* 200–201, 157–168.
- Kay, S.M., Coira, B., Viramonte, J., 1994. Young mafic back arc volcanic rocks as indicators of continental lithospheric delamination beneath the Argentine Puna plateau, central Andes. *Journal of Geophysical Research* 99 (B12), 24323–24339.
- Kay, S.M., Mpodozis, C., 2001. Central Andean ore deposits linked to evolving shallow subduction systems and thickening crust. *GSA Today* 11(3), 4–9.
- Kay, S.M., Mpodozis, C., Coira, B., 1999. Neogene magmatism, tectonism, and mineral deposits of central Andes (220 to 330 Latitude). *Geology and ore Deposits of the Central Andes*. Skinner B.J.(ed.). Society of Economic

- Geologists Special Publication 7, 27–59.
- Keith, J.D., Whitney, J.A., Hattori, K., Ballantyne, G.H., Christiansen, E.H., Barr, D.L., Cannan, T.M., Hook, C.J., 1997. The role of magmatic sulfides and mafic alkaline magmas in the Bingham and Tintic mining districts, Utah. *Journal of Petrology* 38, 1679–1690.
- Kelser, S.E., Jones, L.M., Walker, R.L., 1975. Intrusive rocks associated with porphyry copper mineralization in island areas. *Economic Geology* 70, 515–526.
- Kerrick, R., Goldfarb, D., Groves, D., Garwin, S., 2000. The geodynamics of world-class gold deposits: Characteristics, space-time distributions, and origins. *Reviews in Economic Geology* 13, 501–551.
- Kirkham, R.V., 1998. Tectonic and structural features of arc deposits: Metallogeny of Volcanic Arcs, British Columbia Geological Survey, B1–45.
- Kirkham, R.V., Margolis, J., 1995. Overview of the sulphurets area, NW-British Columbia. In: Schroeter TG(ed) *Porphyry deposits of the NW-Cordillera of North America*, Canadian Institute of Mining, Metallurgy and Petroleum, Montreal, pp 473–483 (Can Inst Min Metall Petrol Spec Vol 46).
- Kirkham, R.V., Sinclair, W.D., 1996. Porphyry copper, gold, molybdenum, tungsten, tin, silver. In: Eckstrand OR, Sinclair WD, Thorpe RI (eds) *Geology of Canadian mineral deposit types*. Geological Survey of Canada, Ottawa, pp 405–430 (Geol Canada 8).
- Lang, J.R., Stanley, C.R., Thompson, J.F.H., Dunne, K.P.E., 1995. Na–K–Ca magmatic–hydrothermal alteration in alkalic porphyry Cu–Au deposits, British Columbia. *Mineralogical Association of Canada Short Course* 23, 339–366.
- Lang, J.R., Titley, S.P., 1998. Isotopic and geochemical characteristics of Laramide magmatic systems in Arizona and implications for the genesis of porphyry copper deposits. *Economic Geology* 98, 138–170.
- Lee, C.A., Luffi, P., Chin, E.J., Bouchet, R., Dasgupta, R., Morton, D.M., Le Roux, V., Yin, Q.Z., Jin, D., 2012. Copper systematics in arc magmas and implications from crust–mantle differentiation. *Science* 336, 64–68.
- Lee, H.Y., Chung, S.L., Lo, C.H., Ji, J., Lee, T.Y., Qian, Q., Zhang, Q., 2009. Eocene Neotethyan slab breakoff in southern Tibet inferred from the Linzizong volcanic record. *Tectonophysics* 477, 20–35.
- Leech, M.L., 2001. Arrested orogenic development: eclogitization, delamination, and tectonic collapse. *Earth and Planetary Science Letters* 185, 149–159.
- Li, J.X., Qin, K.Z., Li, G.M., Xiao, B., Chen, L., Zhao, J.X., 2011. Post-collisional ore-bearing adakitic porphyries from Gangdese porphyry copper belt, southern Tibet: melting of thickened juvenile arc lower crust. *Lithos* 126, 265–277.
- Lin, W., Zhang, Y.Q., Liang, H.Y., Xie, Y.W., 2004. Petrochemistry and SHRIMP U–Pb zircon age of the Chongjiang ore-bearing porphyry in the Gangdese porphyry belt. *Geochimica* 33, 585–592 (in Chinese with English abstract).
- Liu, C.Z., Wu, F.Y., Chung, S.L., Zhao, Z.D., 2011. Fragments of hot and metasomatized mantle lithosphere in Middle Miocene ultrapotassic lavas, southern Tibet. *Geology* 39, 923–926.
- Lu, Y.J., Kerrich, R., Kemp, A.I.S., McCuaig, T.C., Hou, Z.Q., Hart, C.J.R., Li, Z.X., Cawood, P.A., Bagas, L., Yang, Z.M., Cliff, J., Belousova, E.A., Jourdan, F., Evans, N.J., 2013. Intracontinental Eocene–Oligocene

- porphyry Cu mineral systems of Yunnan, western Yangtze Craton, China: Compositional characteristics, sources, and implications for continental collision metallogeny. *Economic Geology* 108, 1541–1576.
- Ma, H.W., 1990. Granitoid and Mineralization of the Yulong Porphyry Copper Belt in Eastern Tibet. Press of China University of Geosciences, Beijing. 157 pp (Chinese with English abstract).
- Mahéo, G., Guillot, S., Blichert-Toft, J., Rolland, Y., Pêcher, A., 2002. A slab breakoff model for the Neogene thermal evolution of South Karakorum and South Tibet. *Earth and Planetary Science Letters* 195, 45–58.
- Mamani, M., Worner, G., Sempere, T., 2010. Geochemical variations in igneous rocks of the central Andean orocline (13° S to 18° S): Tracing crustal thickening and magma generation through time and space. *Geological Society of America* 122, 162–182.
- Maria, A.H., Luhr, J.F., 2008. Lamprophyres, basanites, and basalts of the western Mexican volcanic belt; volatile contents and a vein-wallrock melting relationship. *Journal of Petrology* 49, 2123–2156.
- Martin, H., 1986. Effect of steeper Archean geothermal gradient on geochemistry of subduction-zone magmas. *Geology* 14, 753–756.
- Maughan, D.T., Keith, J.D., Christiansen, E.H., Pulsipher, T., Hattori, K., Evans, N.J., 2002. Contributions from mafic alkaline magmas to the Bingham porphyry Cu-Au-Mo deposit, Utah, USA. *Mineralium Deposita* 37, 14–37.
- McInnes, B.I.A., Gregoire, M., Binns, R.A., Herzig, P.M., Hannington, M.D., 2001. Hydrous metasomatism of oceanic sub-arc mantle, Lihir, Papua New Guinea: petrology and geochemistry of fluid-metasomatised mantle wedge xenoliths. *Earth and Planetary Science Letters* 188, 169–183.
- Miller, C., Schuster, R., Klötzli, U., Frank, W., Purtscheller, F., 1999. Post-collisional potassic and ultra-potassic magmatism in SW Tibet, geochemical, Sr-Nd-Pb-O isotopic constraints for mantle source characteristics and petrogenesis. *Journal of Petrology* 83, 5361–5375.
- Mitchell, A.H.G., Garson, M.S., 1972. Relationship of porphyry copper and circum-pacific deposits to paleo-Benioff zones. *Institute of Mining and Metallurgy Transactions (Sect. B Applied Earth Science)* 81, B10–B25.
- Mo, X., Hou, Z., Niu, Y., Dong, G., Qu, X., Zhao, Z., Yang, Z., 2007. Mantle contributions to crustal thickening during continental collision: Evidence from Cenozoic igneous rocks in southern Tibet. *Lithos* 96, 225–242.
- Mo, X., Niu, Y., Dong, G., Zhao, Z., Hou, Z., Su, Z., Ke, S., 2008. Contribution of syncollisional felsic magmatism to continental crust growth: A case study of the Paleogene Linzizong volcanic Succession in southern Tibet. *Chemical Geology* 250, 49–67.
- Müller, D., Forrestal, P., 1998. The shoshonite porphyry Cu-Au association at Bajo de la Alumbrera, Catamarca Province, Argentina. *Mineralogy and Petrology* 64, 47–64.
- Müller, D., Forrestal, P., 2000. The shoshonite porphyry Cu-Au association at Bejo de la Alumbrera, Catamarca Province, Argentina: a reply. *Mineralogy and Petrology* 68, 305–308.
- Müller, D., Groves, D.I., 1993. Direct and indirect associations between potassic igneous rocks shoshonites and gold-copper deposits. *Ore Geology Review* 8, 383–406.
- Müller, D., Rock, N.M.S., Groves, D.I., 1992. Geochemical discrimination between shoshonitic and potassic

- volcanic rocks in different tectonic settings: a pilot study. *Mineralogy and Petrology* 46, 259–289.
- Mungall, J.E., 2002. Roasting the mantle: slab melting and the genesis of major Au and Au-rich Cu deposits. *Geology* 30, 915–918.
- Mungall, J.E., Hanley, J.J., Arndt, N.T., Debecdelievre, A., 2006. Evidence from meimechites and other low-degree mantle melts for redox controls on mantle-crust fractionation of platinum-group elements. *Proceedings of the National Academy of Sciences of the United States of America* 103, 12695–12700.
- Muntean, J.L., Einaudi, M., 2000. Porphyry gold deposits of the Refugio District, Maricunga belt, Northern Chile. *Economic Geology* 95, 1445–1472.
- Noll, P.D., Newsom, H.E., Leeman, W.P., Ryan, J.G., 1996. The role of hydrothermal fluids in the production of subduction zone magmas: evidence from siderophile and chalcophile trace elements and boron. *Geochimica et Cosmochimica Acta* 60, 587–611.
- Owens, T.J., Zandt, G., 1997. Implications of crustal property variations for models of Tibetan plateau evolution. *Nature* 387, 37–43.
- Oyarzun, R., Márquez, A., Lillo, J., López, I., Rivera S., 2001. Giant versus small porphyry copper deposits of Cenozoic age in northern Chile: Adakitic versus normal calc-alkaline magmatism. *Mineralium Deposita* 36, 794–798.
- Oyarzun, R., Márquez, A., Lillo, J., López, I., Rivera S., 2002. Reply to Discussion on “Giant versus small porphyry copper deposits of Cenozoic age in northern Chile: adakitic versus normal calc-alkaline magmatism” by Oyarzun, R., Márquez, A., Lillo, J., López, I., Rivera, S., (*Mineralium Deposita* 36, 794–798, 2001). *Mineralium Deposita* 37, 795–799.
- Parkinson, I.J., Arculus, R.J., 1999. The redox state of subduction zones: insights from arc-peridotites. *Chemical Geology* 160, 409–423.
- Petford, N., Atherton, M., 1996. Na-rich partial melts from newly underplated basaltic crust: the Cordillera Blanca Batholith, Peru. *Journal of Petrology* 37, 1491–1521.
- Pettke, T., Oberli, F., Heinrich, C.A., 2010. The magma and metal source of giant porphyry-type ore deposits, based on lead isotope microanalysis of individual fluid inclusions. *Earth and Planetary Science Letters* 296, 267–277.
- Pokrovski, G.S., Borisova, A.Y., Harrichoury, J.C., 2008. The effect of sulfur on vapor-liquid fractionation of metals in hydrothermal systems. *Earth and Planetary Science Letters* 266, 345–362.
- Pokrovski, G.S., Roux, J., Harrichoury, J.C., 2005. Fluid density control on vapor-liquid partitioning of metals in hydrothermal systems. *Geology* 33, 657–660.
- Prelević, D., Brüggemann, G., Barth, M., Božović, M., Cvetković, V., Foley, S.F., Maksimović, Z., 2014. Os-isotope constraints on the dynamics of orogenic mantle: The case of the Central Balkans. *Gondwana Research* (2014), <http://dx.doi.org/10.1016/j.gr.2014.02.001>.
- Qin, Z.P., Wang, X.W., Tang, J.X., Tang, X.Q., Zhou, Y., Peng, H.J., 2011. Geochemical characteristics and their implications of peraluminous in the Jiama deposit, Tibet. *Journal of Chendou University of Technology* 38, 76–84 (in Chinese with English abstract).

- Qu, X.M., Hou, Z.Q., Huang, W., 2001. Gangdese porphyry copper belt: The second “Yulong” porphyry Cu belt in Tibet? *Mineral Deposits* 20, 355–366 (in Chinese with English abstract).
- Qu, X.M., Hou, Z.Q., Zaw, K., Li, Y.G., 2007. Characteristics and genesis of Gangdese porphyry copper deposits in the southern Tibetan Plateau: preliminary geochemical and geochronological results. *Ore Geology Reviews* 31, 205–223.
- Qu, X.M., Hou, Z.Q., Zaw, K., Mo, X.X., Xu, W.Y., Xin, H.B., 2009. A large-scale copper ore-forming event accompanying rapid uplift of the southern Tibetan Plateau: Evidence from zircon SHRIMP U-Pb dating and LA ICP-MS analysis. *Ore Geology Reviews* 36, 52–64.
- Qu, X.M., Hou, Z.Q., Li, Y.G., 2004. Melt components derived from a subducted slab in late orogenic ore-bearing porphyries in the Gangdese copper belt, southern Tibetan plateau. *Lithos* 74, 131–148.
- Qu, X.M., Hou, Z.Q., Li, Z.Q., 2003. $^{40}\text{Ar}/^{39}\text{Ar}$ ages of porphyries from the Gangdese porphyry Cu belt in south Tibet and implication to geodynamic setting. *Acta Geologica Sinica* 77, 245–252 (in Chinese with English abstract).
- Rabbia, O.M., Hernández, L.B., King, R.W., López-Escobar, L., 2002. Discussion on “Giant versus small porphyry copper deposits of Cenozoic age in northern Chile: adakitic versus normal calcalkaline magmatism” by Oyarzun et al. (*Mineralium Deposita* 36:794–798, 2001). *Mineralium Deposita* 37, 791–794.
- Rapp, R.P., Shimizu, N., Norman, M.D., Applegate, G.S., 1999. Reaction between slab-derived melts and peridotite in the mantle wedge: experimental constraints at 3.8 GPa. *Chemical Geology* 160, 335–356.
- Rapp, R.P., Watson, E.B., 1995. Dehydration melting of metabasalt at 8–32 kbar: implications for continental growth and crust–mantle recycling. *Journal of Petrology* 36, 891–931.
- Redwood, S.D., Rice, C.M., 1997. Petrogenesis of Miocene basic shoshonitic lavas in the Bolivian Andes and implications for hydrothermal gold, silver and tin deposits. *Journal of South American Earth Sciences* 10, 203–221.
- Reich, M., Parada, M.A., Palacios, C., Dietrich, A., Schultz, F., Lehmann, B., 2003. Adakite-like signature of late Miocene intrusions at the Los Pelambres giant porphyry copper deposit in the Andes of central Chile: metallogenic implication. *Mineralium Deposita* 38, 876–885.
- Richards, J.P., 1995. Alkalic-type epithermal gold deposits—a review. In: Thompson, J.F.H. (Ed.), *Magma, Fluids, and Ore Deposits*. Short Course Series, 23. Mineralogical Association of Canada, pp. 367–400. ch. 17.
- Richards, J.P., 2002. Discussion on “Giant versus small porphyry copper deposits of Cenozoic age in northern Chile: adakitic versus normal calc-alkaline magmatism” by Oyarzun et al. (*Mineralium Deposita* 36:794–798, 2001). *Mineralium Deposita* 37, 788–790.
- Richards, J.P., 2003. Tectono-magmatic precursors for porphyry Cu-(Mo-Au) deposit formation. *Economic Geology* 96, 1515–1533.
- Richards, J.P., 2009. Postsubduction porphyry Cu-Au and epithermal Au deposits: products of remelting of subduction-modified lithosphere. *Geology* 37, 247–250.
- Richards, J.P., 2011a. High Sr/Y arc magmas and porphyry Cu \pm Mo \pm Au deposits: just add water. *Economic Geology* 106, 1075–1081.

- Richards, J.P., 2011b. Magmatic to hydrothermal metalfluxes in convergent and collided margins. *Ore Geology Reviews* 40, 1–26.
- Richards, J.P., 2013. Giant ore deposits formed by optimal alignments and combinations of geological processes. *Nature Geoscience* 6 (11), 911–916.
- Richards, J.P., 2014. Tectonic, magmatic, and metallogenic evolution of the Tethyan orogen: From subduction to collision. *Ore Geology Reviews* (2014), doi.org/10.1016/j.oregeorev.2014.11.009
- Richards, J.P., Boyce, A.J., Pringle, M.S., 2001. Geologic evolution of the Escondida area, northern Chile: A model for spatial and temporal location of porphyry Cu mineralization. *Economic Geology* 96, 271–306.
- Richards, J.P., Kerrich, B., 2007. Adakite-like rocks: their diverse origins and questionable role in metallogenesis. *Economic Geology* 102, 537–576.
- Richards, J.P., Spell, T., Rameh, E., Raziq, A., Fletcher, T., 2012. High Sr/Y magmas reflect arc maturity, high magmatic water content, and porphyry Cu ± Mo ± Au potential: examples from the Tethyan Arcs of Central and Eastern Iran and Western Pakistan. *Economic Geology* 107, 295–332.
- Rock, N.M.S., 1987. The nature and origin of lamprophyres: an overview. In: Fitton JG, Upton BGJ (eds) *Alkaline igneous rocks*. Geological Society, London, pp 191–226 (Geol. Soc. Lond. Spec. Publ. 30).
- Rock, N.M.S., Taylor, W.R., Perring, C.S., 1990. Lamprophyres-what are lamprophyres? In: Ho SE, Groves DI, Bennett JM (eds) *Gold deposits of the Archaean Yilgarn Block, Western Australia: nature, genesis and exploration guides*. Geology Key Centre & University Extension, The University of Western Australia, Perth, pp 128–135 (Geol Dept & Univ Extension, Univ West Austr, Publ 20)
- Rudnick, R., Gao, S., 2003. Composition of the continental crust. In: Rudnick, R.L. (Ed.) *The Crust*, vol. 3. *Treatise on Geochemistry* (Holland, H.D., Turekian, K.K. (Eds.)). Elsevier-Pergamon, Oxford 1–64.
- Rui, Z.Y., Hou, Z.Q., Li, G.M., Liu, B., Zhang, L.S., Wang, L.S., 2006. A genetic model for the Gandesi porphyry copper deposits. *Geological Review* 52, 459–466.
- Rui, Z.Y., Huang, C.K., Qi, G.M., Xu, J., Zhang, M.T., 1984. *The Porphyry Cu (-Mo) Deposits in China*. Beijing: Geological Publishing House. 1–350 (in Chinese with English abstract).
- Rui, Z.Y., Li, G.M., Zhang, L.S., Wang, L.S., 2004. The response of porphyry copper deposits to important geological events in Xizang. *Earth Science Frontiers* 11, 145–152 (in Chinese with English abstract).
- Saadat, S., Stern, C.R., Moradian, A., 2014. Petrochemistry of ultrapotassic tephrites and associated cognate plutonic xenoliths with carbonatite affinities from the late Quaternary Qa'le Hasan Ali maars, central Iran. *Journal of Asian Earth Sciences* 89, 108–122.
- Sajona, F.G., Maury, R.C., 1998. Association of adakites with gold and copper mineralization in the Philippines. *Comptes Rendus de l'Académie des Sciences - Series IIA - Earth and Planetary Science* 326, 27–34.
- Sandeman, H.A., Clark, A.H., 2004. Commingling and mixing of S-type peraluminous, ultrapotassic and basaltic basaltic magmas in the Cayconi volcanic field, Cordillera de Carabaya, SE Peru. *Lithos* 73, 187–213.
- Schutte, P., Chiaradia, M., Beate, B., 2010. Petrogenetic evolution of arc magmatism associated with late Oligocene to late Miocene porphyry-related Ore Deposits in Ecuador. *Economic Geology* 105, 1243–1270.
- Seo, J.H., Guillong, M., Heinrich, C.A., 2009. The role of sulfur in the formation of magmatic-hydrothermal

- copper-gold deposits. *Earth and Planetary Science Letters* 282, 323–328.
- Shafiei, B., Haschke, M., Shahabpour, J., 2009. Recycling of orogenic arc crust triggers porphyry Cu mineralization in Kerman Cenozoic arc rocks, southeastern Iran. *Mineralium Deposita* 44, 265–283.
- Sillitoe, R.H., 1991. Gold metallogeny of Chile: an introduction. *Economic Geology* 86, 1187–1205.
- Sillitoe, R.H., 1972. A plate tectonic model for the origin of porphyry copper deposits. *Economic Geology* 67, 184–197.
- Sillitoe, R.H., 1973. The tops and bottoms of porphyry copper deposits: *Economic Geology* 68, 799–815.
- Sillitoe, R.H., 1997. Characteristics and controls of the largest porphyry copper-gold and epithermal gold deposits in the circum-Pacific region. *Australian Journal of Earth Sciences* 44, 373–388
- Sillitoe, R.H., 1998. Major regional factors favouring large size, high hypogene grade, elevated gold content and supergene oxidation and enrichment of porphyry copper deposits, in Porter, T.M., ed., *Porphyry and hydrothermal copper and gold deposits: A global perspective*: Adelaide, Australian Mineral Foundation, p. 21–34.
- Sillitoe, R.H., 2000. Gold-rich porphyry deposits: Descriptive and genetic models and their role in exploration and discovery: *Reviews in Economic Geology* 13, 315–345.
- Sillitoe, R.H., 2002. Some metallogenic features of gold and copper deposits related to alkaline rocks and consequences for exploration. *Mineralium Deposita* 37, 4–13.
- Sillitoe, R.H., 2005. Supergene oxidized and enriched porphyry copper and related deposits. *Economic Geology* 100th Anniversary Volume, 723–768.
- Sillitoe, R.H., 2010. Porphyry copper systems. *Economic Geology* 105, 3–41.
- Sillitoe, R.H., Camus, F., 1991. A special issue devoted to the gold deposits in the Chilean Andes-preface. *Economic Geology* 86, 1153–1154.
- Simon, A.C., Frank, M.R., Pettke, T., Candela, P.A., Piccoli, P.M., Heinrich, C.A., 2005. Gold partitioning in melt-vapor-brine systems. *Geochimica et Cosmochimica Acta* 69, 3321–3335.
- Simon, A.C., Pettke, T., Candela, P.A., Piccoli, P.M., Heinrich, C.A., 2006. Copper partitioning in a melt-vapor-brine-magnetite-pyrrhotite assemblage. *Geochimica et Cosmochimica Acta* 70, 5583–5600.
- Sinclair, W.D., 2007. Porphyry deposits, in Goodfellow, W.D., ed., *Mineral Deposits of Canada: A Synthesis of Major Deposit-Types, District Metallogeny, the Evolution of Geological Provinces, and Exploration Methods*: Geological Association of Canada, Mineral Deposits Division, Special Publication No. 5, p. 223–243.
- Skewes, M.A., Stern, C.R., 1995. Genesis of the giant late Miocene to Pliocene copper deposits of central Chile in the context of Andean magmatic and tectonic evolution. *International Geology Review* 37, 893–909.
- Skjerlie, K.P., Patino-Douce, A.E., 2002. The fluid-absent partial melting of a zoisite-bearing quartz eclogite from 1.0 to 3.2 GPa; implications for melting in thickened continental crust and for subduction-zone processes. *Journal of Petrology* 43, 291–314.
- Solomon, M., 1990. Subduction, arc reversal, and the origin of porphyry copper-gold deposits in island arcs. *Geology* 18, 630–633.
- Spicer, R.A., Harris, N.B.W., Widdowson, M., Herman, A.B., Guo, S., Valdes, P.J., Wolfek, J.A., Kelley, S.P., 2003.

- Constant elevation of southern Tibet over the past 15 million years. *Nature* 421, 622–624.
- Stavast, W.J.A., Keith, J.D., Christiansen, E.H., Dorais, M.J., Tingey, D., Larocque, A., Evans, N., 2006. The fate of magmatic sulfides during intrusion or eruption, Bingham and Tintic Districts, Utah. *Economic Geology* 101, 329–345.
- Stern, C.R., Funk, J.A., Skewes, M.A., Arevalo, A., 2007. Magmatic anhydrite in plutonic rocks at the El Teniente Cu-Mo deposit, Chile, and the role of sulfur- and copper-rich magmas in its formation. *Economic Geology* 102, 1335–1344.
- Stern, C.R., Skewes, M.A., Arévalo, A., 2010. Magmatic evolution of the Giant El Teniente Cu-Mo deposit, Central Chile. *Journal of Petrology* 52, 1591–1671.
- Sun, S.S., 1982. Chemical composition and origin of the Earth's primitive mantle. *Geochimica et Cosmochimica Acta* 46, 179–192.
- Sun, S.S., McDonough, W.F., 1989. Chemical and isotopic systematics of oceanic basalts: implications for mantle composition and processes. Geological Society, London, Special Publication 42, 313–345.
- Sun, W., Ling, M.X., Chung, S.L., Ding, X., Yang, X.Y., Liang, H.Y., Fan, W.M., Goldfarb, R., Yin, Q.Z., 2012. Geochemical constraints on adakites of different origins and copper mineralization. *The Journal of Geology* 120, 105–120.
- Sun, W., Zhang, H., Ling, M.X., Ding, X., Chung, S.L., Zhou, J., Yang, X.Y., Fan, W., 2011. The genetic association of adakites and Cu–Au ore deposits. *International Geology Review* 53, 691–703.
- Sun, W.D., Arculus, R.J., Bennett, V.C., Eggins, S.M., Binns, R.A., 2003. Evidence for rhenium enrichment in the mantle wedge from submarine arc-like volcanic glasses (Papua New Guinea). *Geology* 31, 845–848.
- Sun, W.D., Arculus, R.J., Kamenetsky, V.S., Binns, R.A., 2004. Release of gold-bearing fluids in convergent margin magmas prompted by magnetite crystallization. *Nature* 431, 975–978.
- Sun, W.D., Huang, R.F., Li, H., Hu, Y.B., Zhang, C.C., Sun, S.J., Zhang, L.P., Ding, X., Li, C.Y., Zartman, R.E., Ling, M.X., 2014. Porphyry deposits and oxidized magmas. *Ore Geology Reviews* 65, 97–131.
- Sun, W.D., Liang, H.Y., Ling, M.X., Zhan, M.Z., Ding, X., Zhang, H., Yang, X.Y., Li, Y.L., Ireland, T.R., Wei, Q.R., Fang, W.M., 2013. The link between reduced porphyry copper deposits and oxidized magmas. *Geochimica et Cosmochimica Acta* 103, 263–275.
- Sun, W.D., Ling, M.X., Yang, X.Y., Fan, W.M., Ding, X., Liang, H.Y., 2010. Ridge subduction and porphyry copper-gold mineralization: an overview. *Science China (Earth Sciences)* 53, 475–484.
- Tang, R.L., Luo, H.S., 1995. The Geology of Yulong Porphyry Copper (molybdenum) Ore Belt, Xizang (Tibet). Geological Publishing House, Beijing. 320 pp (in Chinese with English abstract).
- Tapponnier, P., Xu, Z., Roger, F., Meyer, B., Arnaud, N., Wittlinger, G., Yang, J., 2001. Oblique stepwise rise and growth of the Tibet Plateau. *Science* 294, 1671–1677.
- Thiéblemont, D., Stein, G., Lescuyer, J.L., 1997. Gisements épithermaux et porphyriques: la connexion adakite: C.R. Acad. Sci. Paris, Sciences de la terre et des planètes/Earth and Planetary Sciences 325, 103–109.
- Tommasini, S., Avanzinelli, R., Conticelli, S., 2011. The Th/La and Sm/La conundrum of the Tethyan realm lamproites. *Earth and Planetary Science Letters* 301, 469–478.

- Turner, S., Arnaud, N.O., Liu, J., Roger, N., Hawkesworth, C., Harris, N., Kelley, S., 1996. Post-collision, shoshonitic volcanism on the Tibetan plateau, implications for convective thinning of the lithosphere and source of ocean island basalts. *Journal of Petrology* 37, 45–71.
- Turner, S., Hawkesworth, C., Liu, J., Rogers, N., Kelley, S., van Calsteren, P., 1993. Timing of Tibetan uplift constrained by analysis of volcanic rocks. *Nature* 364, 50–53.
- Ulrich, T., Heinrich, C.A., 2001. Geology and alteration geochemistry of the porphyry Cu-Au deposit at Bajo de la Alumbrera, Argentina. *Economic Geology* 96, 1719–1742.
- Vila, T., Sillitoe, R.H., 1991. Gold-rich porphyry system in the Maricunga Belt, Northern Chile. *Economic Geology* 86, 1238–1260.
- Vry, V.H., Wilkinson, J.J., Seguel, J., Millán, J., 2010. Multistage intrusion, Brecciation, and Veining at El Teniente, Chile: evolution of a nested porphyry system. *Economic Geology* 105, 119–153.
- Wallace, P., Carmichael, I.S.E., 1989. Minette lavas and associated leucitites from the western front of the Mexican volcanic belt: petrology, chemistry, and origin. *Contributions to Mineralogy and Petrology* 103, 470–492.
- Wallace, P.J., Edmonds, M., 2011. The sulfur budget in magmas: Evidence from melt inclusions, submarine glasses, and volcanic gas emissions. *Reviews in Mineralogy and Geochemistry* 73, 215–246.
- Wang, B.D., Chen, J.L., Xu J.F., Wang, L.Q., 2014. Geochemical and Sr-Nd-Pb-Os isotopic compositions of Miocene ultrapotassic rocks in southern Tibet: petrogenesis and implications for the regional tectonic history. *Lithos* 208–209, 237–250.
- Wang, B.D., Xu, J.F., Chen, J.L., Zhang, X.G., Wang, L.Q., Xia, B.B., 2010. Petrogenesis and geochronology of the ore-bearing porphyritic rocks in Tangbula porphyry molybdenum-copper deposit in the eastern segment of the Gangdese metallogenic belt. *Acta Petrologica Sinica* 26, 1820–1832 (in Chinese with English abstract).
- Wang, L.L., Mo, X.X., Li, B., Dong, G.C., Zhao, Z.D., 2006. Geochronology and geochemistry of the ore-bearing porphyry in Qulong Cu (Mo) ore deposit, Tibet. *Acta Petrologica Sinica* 24, 1001–1008 (in Chinese with English abstract).
- Wang, Q., Tang, G.J., Jia, X.H., Zi, F., Jiang, Z.Q., Xu, J.F., Zhang, Z.H., 2008. The metalliferous mineralization associated with adakitic rocks. *Geological Journal of China Universities* 14, 350–364 (in Chinese with English abstract).
- Wang, R., Richards, J.P., Hou, Z.Q., Yang, Z.M., 2014a. Extent of underthrusting of the Indian plate beneath Tibet controlled of Miocene porphyry Cu-Mo ± Au deposits. *Mineralium Deposita* 49, 165–173.
- Wang, R., Richards, J.P., Hou, Z.Q., Yang, Z.M., DuFrane, S.A., 2014b. Increased magmatic water content—the key to Oligo-Miocene porphyry Cu-Mo ± Au formation in the eastern Gangdese belt, Tibet. *Economic Geology* 109, 1315–1339.
- Wang, Z.H., Liu, Y.L., Liu, H.F., Guo, L.S., Zhang, J.S., Xu, K.F., 2012. Geochronology and geochemistry of the Bangpu Mo-Cu porphyry ore deposit, Tibet. *Ore Geology Reviews* 46, 95–105.
- Williams, H., Turner, S., Kelley, S., Harris, N., 2001. Age and composition of dikes in southern Tibet: new constraints on the timing of east-west extension and its relationship to post-collisional volcanism. *Geology* 29, 339–342.

- Williams, H., Turner, S., Pearce, J.A., Kelley, S.P., Harris, N.B.W., 2004. Nature of the source regions for post-collisional, potassic magmatism in southern and northern Tibet from geochemical variations and inverse trace element modeling. *Journal of Petrology* 45, 555–607.
- Wilson, M., 1989. *Igneous Petrogenesis*. Unwin-Hyman, London. 461 pp.
- Wolf, M.B., Wyllie, P.J., 1991. Dehydration-melting of solid amphibolite at 10 kbar: textural development, liquid interconnectivity and applications to the segregation of magmas. *Mineralogy and Petrology* 44, 151–179.
- Xia, B.B., Xia, B., Wang, B.D., Li, J.F., 2010. Formation time of the Tangbula porphyry Mo-Cu deposit: evidence from SHRIMP zircon U-Pb dating of Tangbula ore-bearing porphyries. *Geotectonica et Metallogenia* 34, 291–297 (in Chinese with English abstract).
- Xia, B.B., Xia, B., Wang, B.D., Zhao, S.R., 2007. Ore-bearing adakitic porphyry in the Middle of Gangdese: thickened lower crustal melting and the genesis of porphyry Cu-Mo deposit. *Geological Science and Technology Information* 26(4), 19–26 (in Chinese with English abstract).
- Yang, Z.M., Hou, Z.Q., White, N.C., Chang, Z.S., Li, Z.Q., Song, Y., 2009. Geology of the postcollisional porphyry copper-molybdenum deposit at Qulong, Tibet. *Ore Geology Reviews* 36, 133–159.
- Yang, Z.M., Hou, Z.Q., Xu, J.F., Bian, X.F., Wang, G.R., Yang, Z.S., Tian, S.H., Liu, Y.C., Wang, Z.L., 2014. Geology and origin of the post-collisional Narigongma porphyry Cu-Mo deposit, southern Qinghai, Tibet. *Gondwana Research* 26, 536–556.
- Zajacz, Z., Halter, W.E., Pettke, T., Guillong, M., 2008. Determination of fluid/melt partition coefficients by LA-ICPMS analysis of co-existing fluid and silicate melt inclusions: controls on element partitioning. *Geochimica et Cosmochimica Acta* 72, 2169–2197.
- Zajacz, Z., Seo, J.H., Candela, P.A., Piccoli, P.M., Tossell, J.A., 2011. The solubility of copper in high-temperature magmatic vapors: a quest for the significance of various chloride and sulfide complexes. *Geochimica et Cosmochimica Acta* 75, 2811–2827.
- Zhao, W.J., Nelson, K.D., 1993. Deep seismic-reflection evidence for continental underthrusting beneath Southern Tibet. *Nature* 366, 557–559.
- Zhao, Z., Mo, X., Dilek, Y., Niu, Y., Depaolo, D., Robinson, P., Zhu, D., Sun, C., Dong, G., Zhou, S., Luo, Z., Hou, Z., 2009. Geochemical and Sr-Nd-Pb-O isotopic compositions of the post-collisional ultrapotassic magmatism in SW Tibet: Petrogenesis and implications for India intra-continental subduction beneath southern Tibet. *Lithos* 113, 190–212.
- Zheng, Y.C., Hou, Z.Q., Li, Q.L., Sun, Q.Z., Liang, W., Fu, Q., Li, W., Huang, K.X., 2012. Origin of Late Oligocene adakitic intrusives in the southeastern Lhasa terrane: Evidence from in situ zircon U-Pb dating, Hf-O isotopes, and whole-rock geochemistry. *Lithos* 148, 296–311.
- Zheng, Y.Y., Gao, S.B., Chen, L.J., Li, G.L., Feng, N.P., Fan, Z.H., Zhang, H.P., Guo, J.C., Zhang, G.Y., 2004. Finding and Significances of Chongjiang Porphyry copper (Molybdenum, Aurum) Deposit, Tibet. *Earth Science-Journal of China University of Geosciences* 29, 333–339 (in Chinese with English abstract).
- Zhu, D.C., Zhao, Z.D., Niu, Y.L., Mo, X.X., Chung, S.L., Hou, Z.Q., Wang, L.Q., Wu, F.Y., 2011. The Lhasa terrane: record of a microcontinent and its histories of drift and growth. *Earth and Planetary Science Letters*

301, 241–255.

Zhu, D.C., Zhao, Z.D., Pan, G.T., Lee, H.Y., Kang, Z.Q., Liao, Z.L., Wang, L.Q., Li, G.M., Dong, G.C., Liu, B., 2009. Early cretaceous subduction-related adakite-like rocks of the Gangdese Belt, southern Tibet: products of slab melting and subsequent melt-peridotite interaction? *Journal of Asian Earth Sciences* 34, 298–309.

ACCEPTED MANUSCRIPT

Figure captions

Fig. 1. (a) Worldwide distribution of porphyry Cu deposits and Cenozoic potassic and ultrapotassic rocks on the Eastern Pacific Rim (EPRIM) and in the world (modified from Müller et al. (1992), and Sillitoe (2010)) and (b) Miocene porphyry Cu mineralization and ultrapotassic rocks in the Gangdese porphyry Cu belt of southern Tibet (modified from Hou et al. (2004, 2009), and Zhao et al. (2009)). Distribution of Cenozoic potassic and ultrapotassic rocks on EPRIM and in the world based on Wallace and Carmichael (1989), Müller et al. (1992), Kay et al. (1994), Carlier et al. (1997), Redwood and Rice (1997), Haschke et al. (2002), Maughan et al. (2002), Carlier and Lorand (2003), Sandeman and Clark (2004), Conticelli et al. (2007), Jiménez and López-Velásquez (2008), Mamani et al. (2010), Gómez-Tuena et al. (2011), Prelević et al. (2014), and Saadat et al. (2014).

Fig. 2. Diagrams showing variations in SiO_2 vs. K_2O (a, b) for mineralized porphyries around the world; CPEPR (Late Cretaceous–Paleogene mineralized porphyries on the eastern Pacific Rim) data from Baldwin and Pearch (1982), Lang and Titley (1998), González-Partida et al. (2003), and Stavast et al. (2006); MPEPR (Miocene mineralized porphyries on the eastern Pacific Rim) data from Müller and Forrestal (1998), Muntean and Einaudi (2000), Ulrich and Heinrich (2001), Reich et al. (2003), Chiaradia et al. (2004), Cannell et al. (2005); Stern et al. (2007, 2010), Vry et al. (2010), and Schutte et al. (2010); MPST (Miocene mineralized porphyries in southern Tibet) data from Hou et al. (2004), Lin et al. (2004), Qu et al. (2004), Zheng et al. (2004), Wang et al. (2006, 2010, 2012), Gao et al. (2007a), Xia et al. (2007, 2010), Li et al. (2011), and Qin et al. (2011); data for late Cretaceous–Paleogene ultrapotassic rocks on the eastern Pacific Rim from Haschke et al. (2002), Maughan et al. (2002), Jiménez and López-Velásquez (2008), and Mamani et al. (2010); data for Miocene ultrapotassic rocks on the eastern Pacific Rim from Wallace and Carmichael (1989), Kay et al. (1994), Carlier et al. (1997), Redwood and Rice (1997), Carlier and Lorand (2003), Maria and Luhe (2008), Sandeman and Clark (2004), and Gómez-Tuena et al. (2011); and data for Miocene ultrapotassic rocks in southern Tibet from Miller et al. (1999), Ding et al. (2003, 2006), Williams et al. (2004), Gao et al. (2007a, b), Zhao et al. (2009), Chen et al. (2012), and Wang et al. (2014).

Fig. 3. Harker diagrams for mineralized porphyries on the eastern Pacific Rim and in southern Tibet; SiO_2 vs. Mg\# diagram based on Wang et al. (2008), and data sources and symbols are as in Fig. 2.

Fig. 4. Diagrams showing variations in trace element concentrations with SiO_2 for mineralized porphyries on the eastern Pacific Rim and in southern Tibet; LC = lower crust, UC = upper crust, values for both are from Rudnick and Gao (2003), and all other data sources and symbols are as in Fig. 2.

Fig. 5. Chondrite-normalized REE (a, b, c) and primitive mantle-normalized multi-element (d, e, f) variation diagrams for porphyry Cu deposits on the eastern Pacific Rim and in southern Tibet; normalizing values are from Sun and McDonough (1989), and all other data sources are as in Fig. 2.

Fig. 6. A $^{87}\text{Sr}/^{86}\text{Sr}_{(i)}$ vs. $\epsilon\text{Nd}_{(t)}$ diagram for porphyry Cu deposits on the eastern Pacific Rim and in southern Tibet; CPEPR data from Lang and Titley (1998); MPEPR data from Reich et al. (2003), Chiaradia et al. (2004), Stern et al. (2010), and Schutte et al. (2010); MPST data from Hou et al. (2004), Lin et al. (2004), Li et al. (2011), Wang et al. (2010), and Qin et al. (2011); data for late Cretaceous–Paleogene ultrapotassic rocks on the eastern Pacific Rim from Maughan et al. (2002); data for Miocene ultrapotassic rocks on the eastern Pacific Rim from Kay et al. (1994), and Gómez-Tuena et al. (2011); and data for Miocene ultrapotassic rocks in southern Tibet from Miller et al. (1999), Ding et al. (2003, 2006), Williams et al. (2004), Gao et al. (2007a, b), Zhao et al. (2009), Chen et al. (2012), and Wang et al. (2014). MORB and marine sediment values are from Hofmann (2003); all data symbols are as in Fig. 2.

Fig. 7. Diagrams showing variations in Sr/Y vs. Y (a, b) and $(\text{La}/\text{Yb})_{\text{N}}$ vs. Yb_{N} (c, d) for porphyry Cu deposits on the eastern Pacific Rim and in southern Tibet; diagrams are after Martin (1986), Drummond and Defant (1990), Petford and Atherton (1996), and Castillo (2012), and all other data sources and symbols are as in Fig. 2.

Fig. 8. Diagrams showing variations in K_2O vs. Mg# (a), Rb vs. Mg# (b), Ba vs. Mg# (c), and Hf/Yb vs. Ce/Yb (d) for porphyry Cu deposits on the eastern Pacific Rim and in southern Tibet; upper and lower crust values are from Rudnick and Gao (2003), and all other data sources and symbols are as in Fig. 2.

Fig. 9. Diagrams showing variations in (a) Ba vs. Nb/Y, (b) Ba/Yb vs. Th/Yb, (c) Th/Yb vs. Sr/Yb, and (d) Th/La vs. Sm/La for porphyry Cu deposits on the eastern Pacific Rim and in southern Tibet; SALATHO is the high Sm/La and Th/La component of Tommasini et al. (2011), upper and lower crust values are from Rudnick and Gao (2003), and all other data sources and symbols are as in Fig. 2.

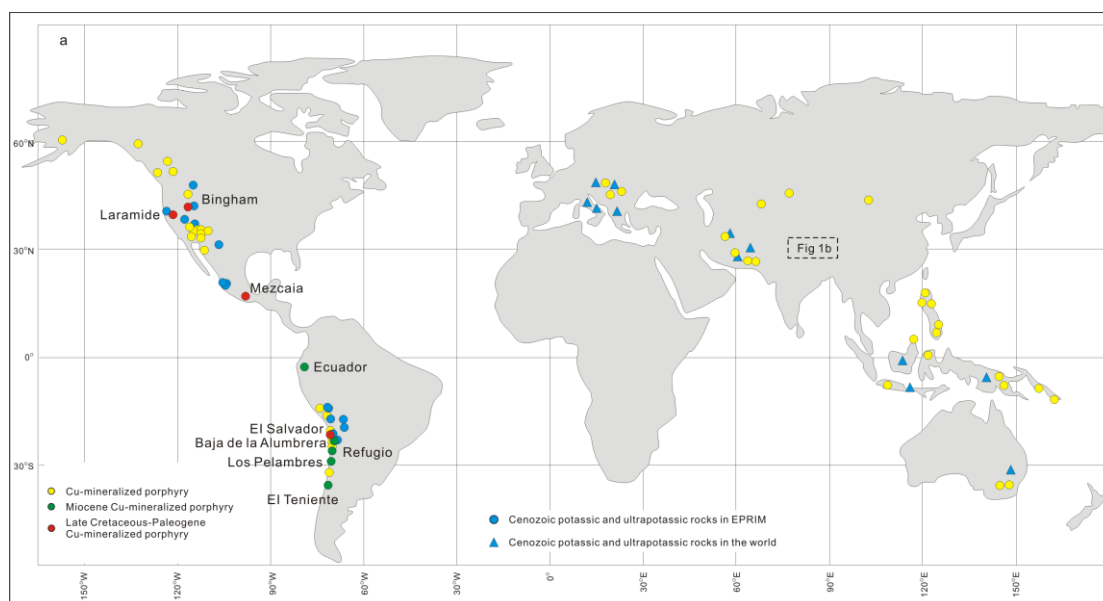


Fig. 1a

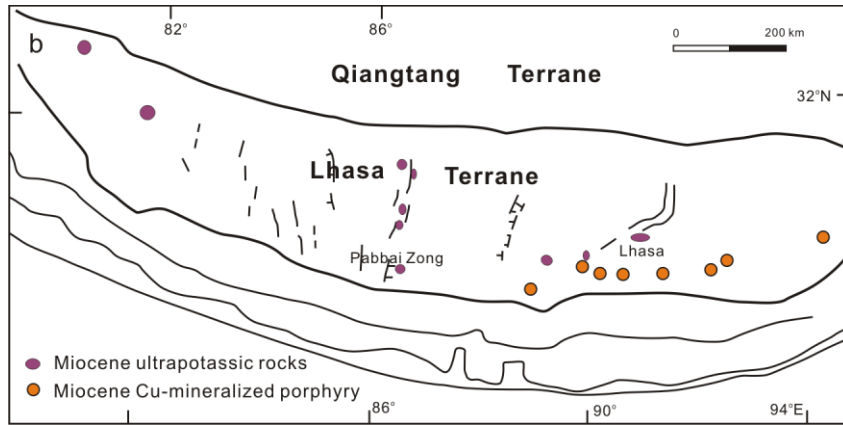


Fig. 1b

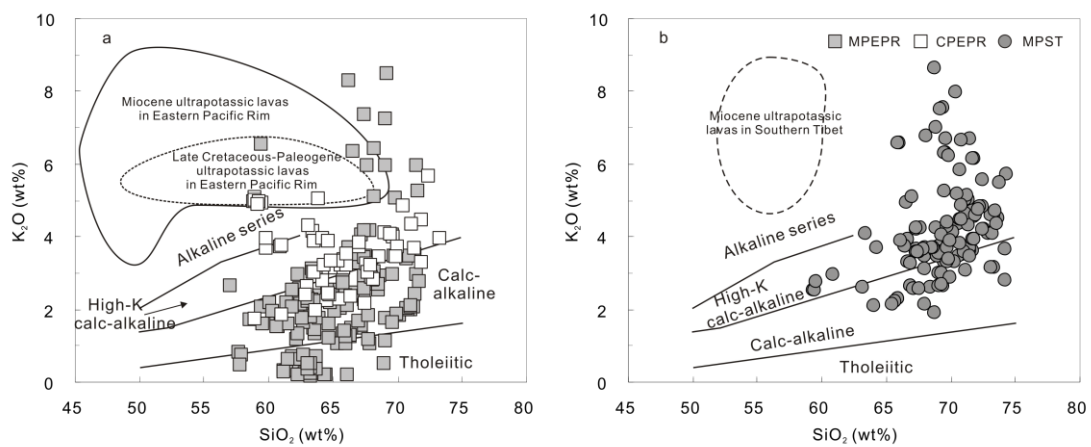


Fig. 2

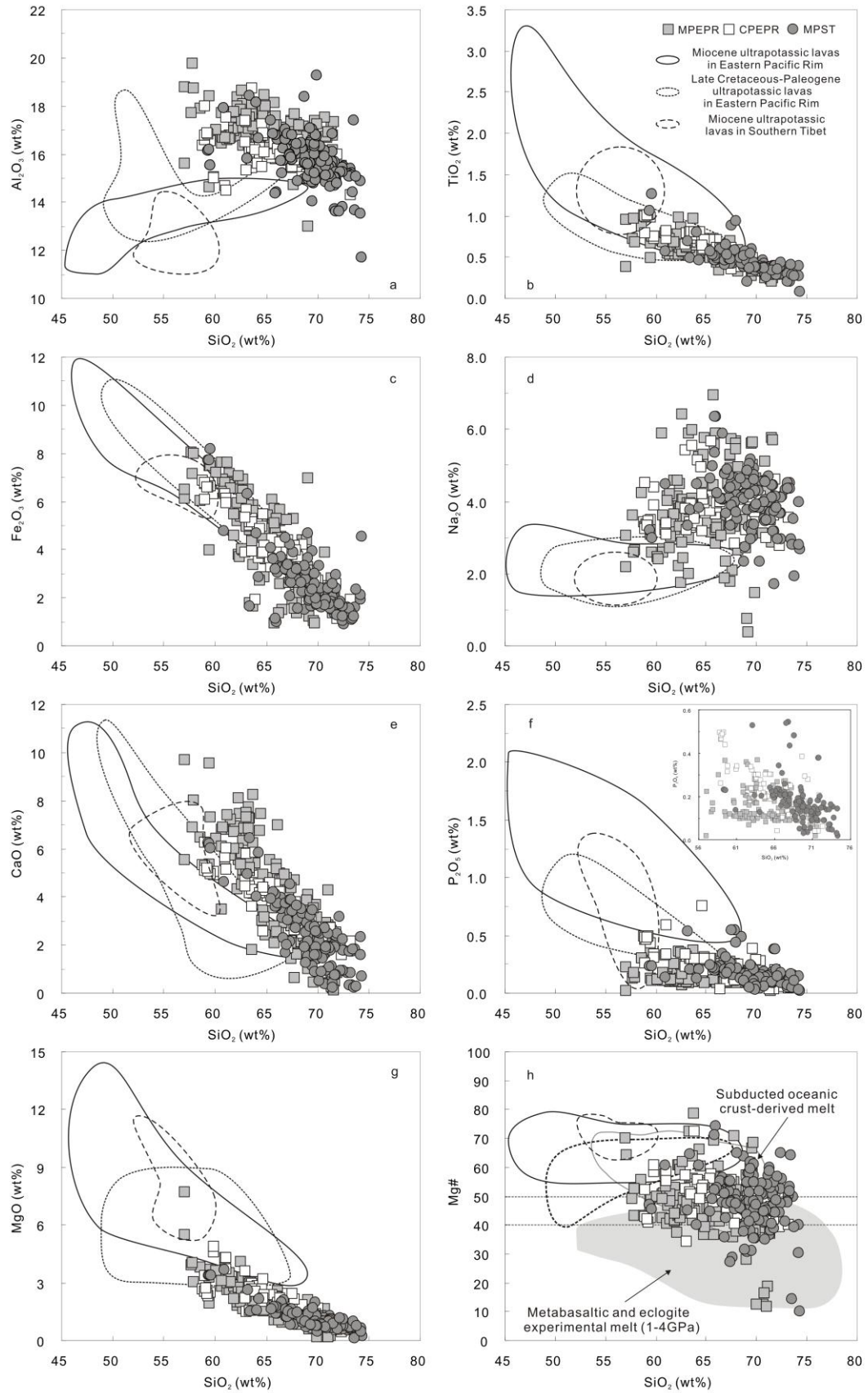


Fig. 3

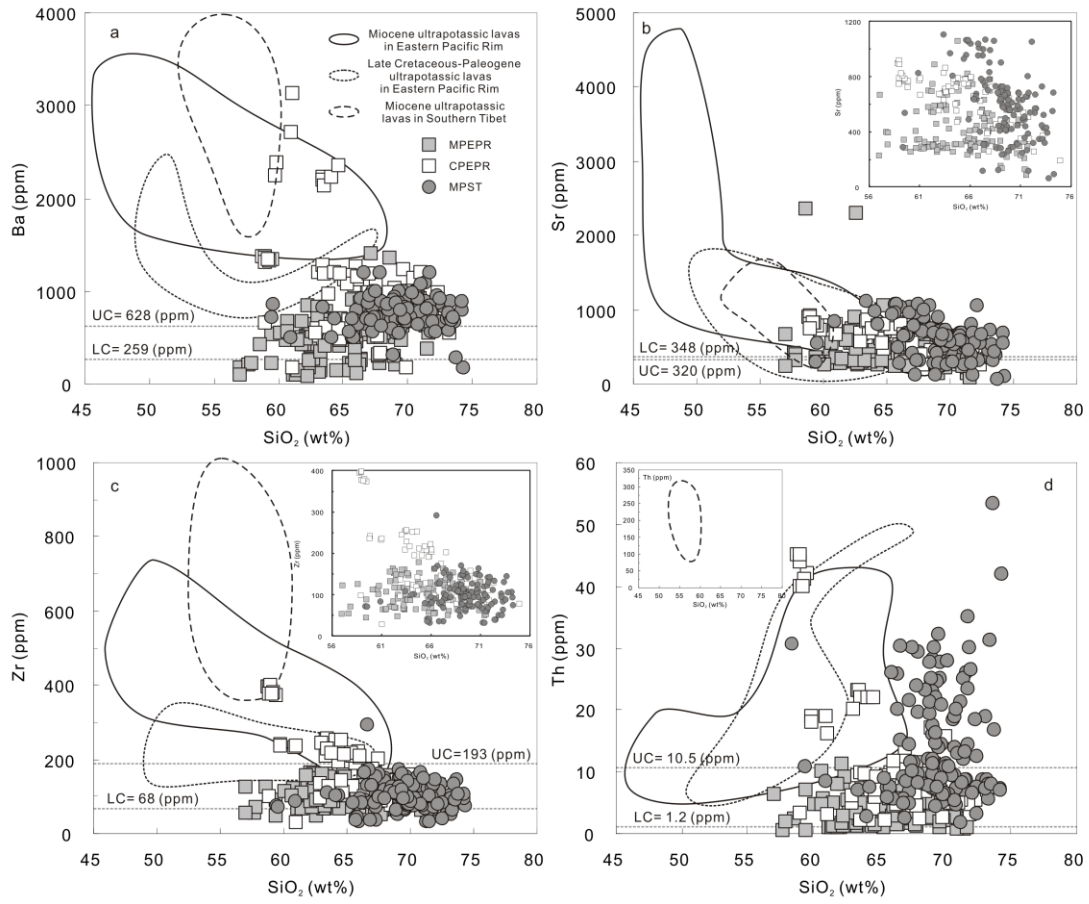


Fig. 4

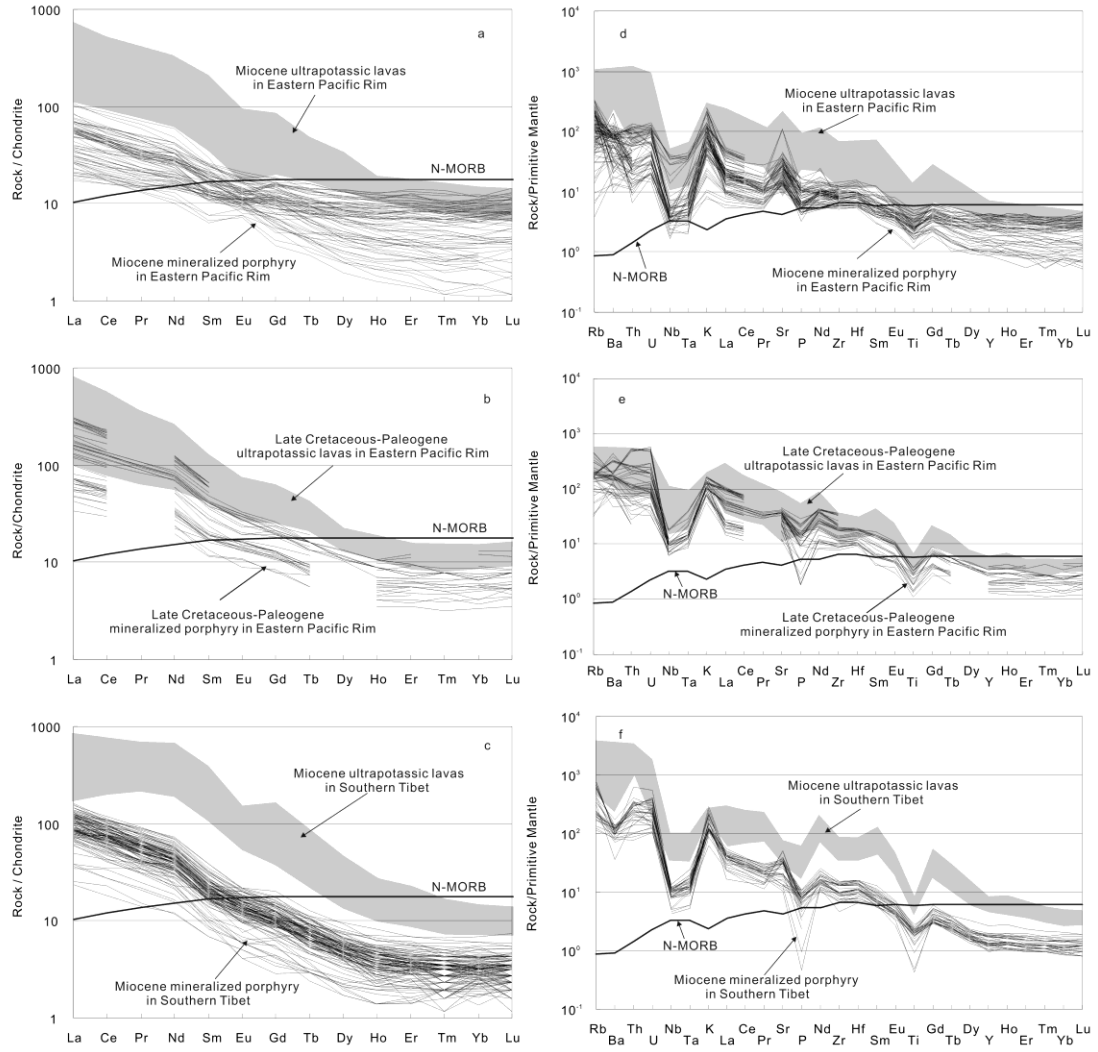


Fig. 5

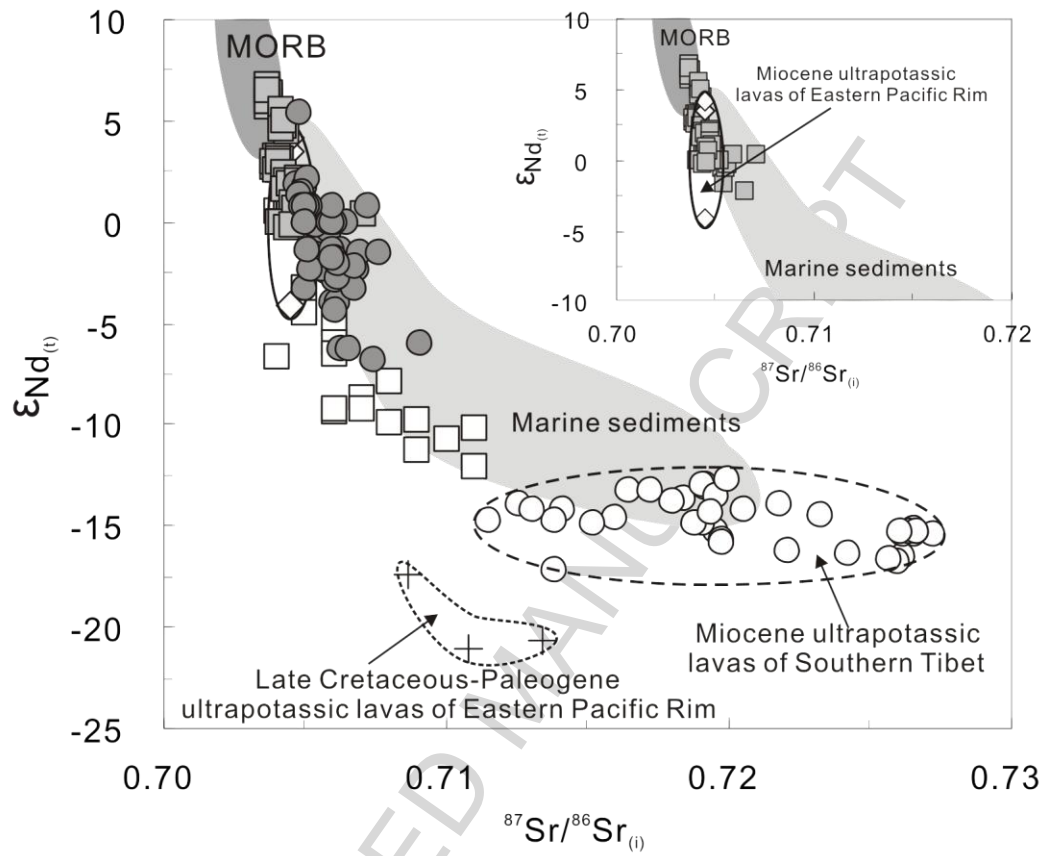


Fig. 6

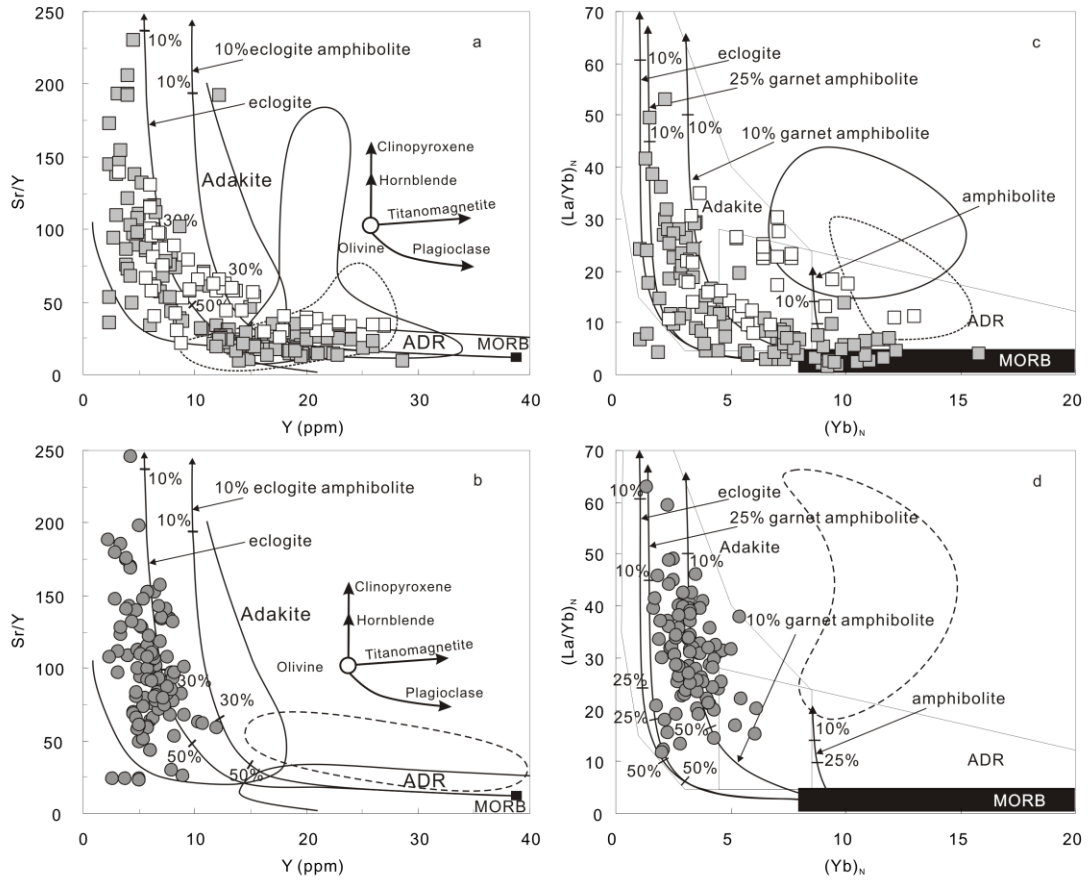


Fig. 7

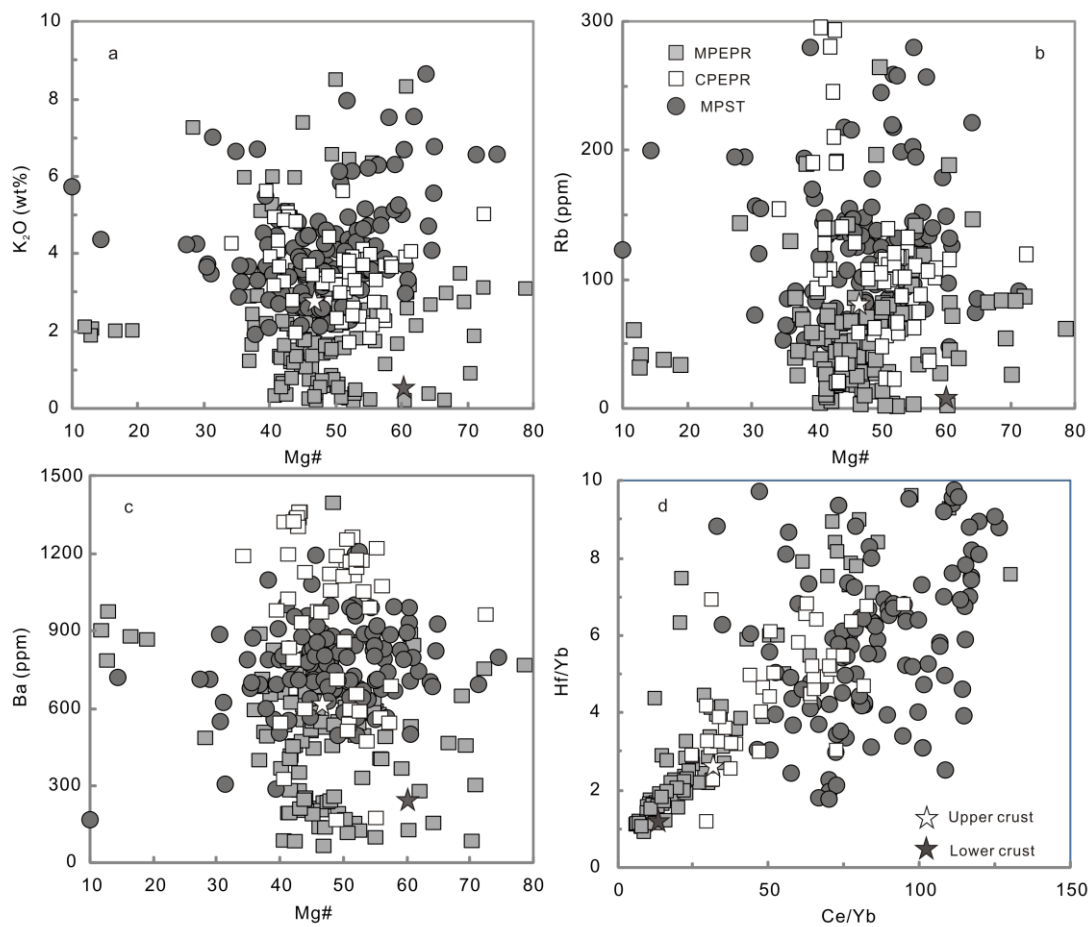


Fig. 8

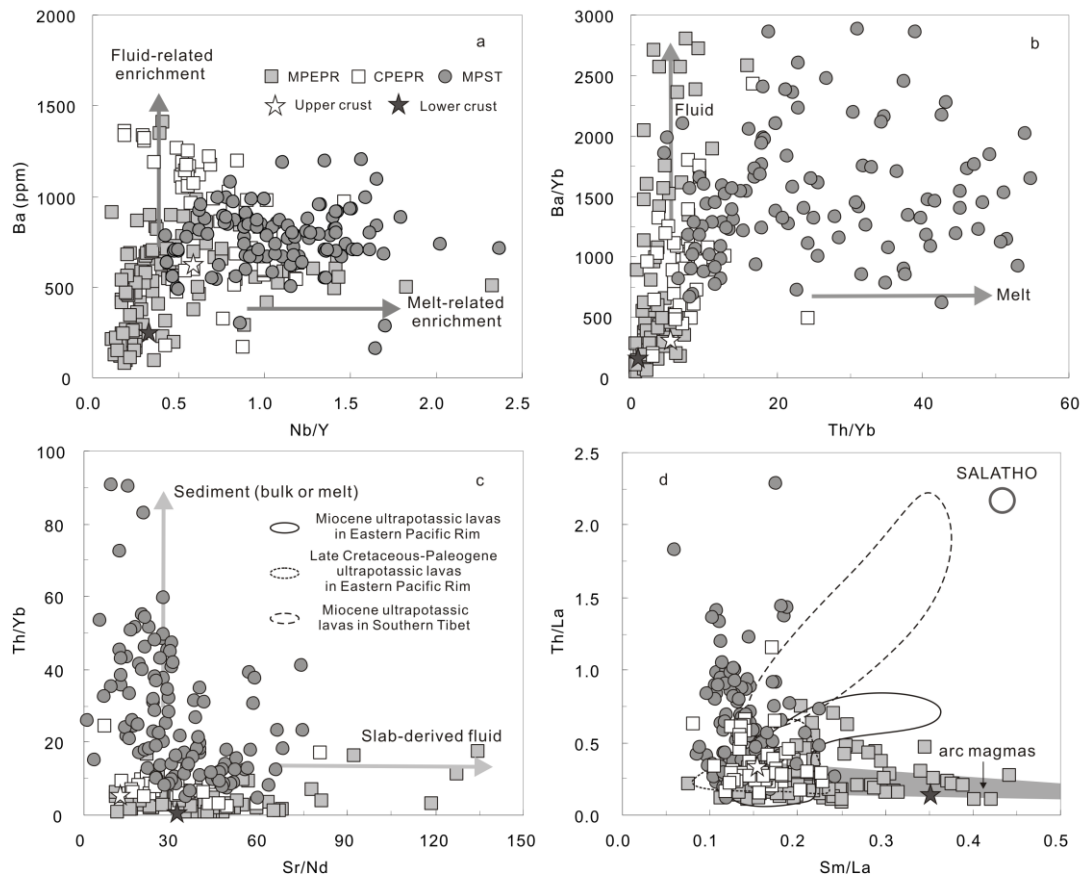


Fig. 9

Table 1. Geochemistry of subduction- and collision-related mineralized Cu porphyries.

Element	Data Range	MPEPR	CPEPR	MPST
Na ₂ O (wt.%)	Range	0.36~8.10	2.76~5.66	1.02~6.36
	Average	3.85 (n=142) *	3.79 (n=62)	3.95 (n=155)
K ₂ O (wt.%)	Range	0.17~8.47	1.73~5.64	1.64~8.65
	Average	2.25 (n=142)	3.61 (n=62)	4.14 (n=155)
K ₂ O/Na ₂ O	Range	0.04~3.50	0.36~1.85	0.43~5.75
	Average	0.60 (n=139)	0.98 (n=61)	1.29 (n=155)
MgO (wt.%)	Range	0.17~4.10	0.43~4.84	0.10~3.66
	Average	2.06 (n=140)	2.20 (n=62)	1.16 (n=155)
Mg#	Range	11.9~72.3	34.2~61.4	10.0~74.5
	Average	47.6 (n=141)	49.5 (n=61)	47.3 (n=155)
Sr (ppm)	Range	87.0~889	193~919	46.4~1106
	Average	418 (n=139)	657 (n=60)	576 (n=137)
Y (ppm)	Range	2.35~28.7	3.28~27.0	2.13~12.5
	Average	12.2 (n=140)	13.6 (n=60)	6.00 (n=137)
Sr/Y	Range	9.41~206	21.8~116	18.1~261
	Average	51.5 (n=138)	55.0 (n=58)	101 (n=135)
(La/Sm) _N	Range	1.46~5.76	2.82~5.44	2.66~7.56
	Average	3.25 (n=100)	4.19 (n=53)	4.76 (n=127)
(Dy/Yb) _N	Range	0.74~2.79	1.51~1.86	0.81~2.02
	Average	1.29 (n=97)	1.68 (n=14)	1.52 (n=127)
(La/Yb) _N	Range	1.67~53.1	7.95~34.7	11.7~63.0
	Average	13.0 (n=100)	18.6 (n=42)	31.1 (n=128)
εNd _(t)	Range	-2.18~6.79	-12.1~-3.19	-6.83~5.70
	Average	2.97 (n=49)	-8.05 (n=18)	-1.32 (n=53)
⁸⁷ Sr/ ⁸⁶ Sr _(i)	Range	0.7037~0.7071	0.7054~0.7145	0.7034~0.7091
	Average	0.7044 (n=53)	0.7076 (n=17)	0.7058 (n=53)

*n = the number of samples = 142 (data sources are as for Fig. 2).